Université de Montréal

Test the ability of axolotl decellularized ECM scaffold to improve skin wound healing in mice

par
Walid Alariba

Département de Stomatologie
Faculté de médecine dentaire
Universbité de Montréal

Mémoire présenté à la Faculté des études supérieures
en vue de l'obtention du grade de
Maîtrise ès Sciences (M.Sc.)
Sciences Buccodentaires

November,2021

Faculté des études supérieures

Ce mémoire intitulé:

Test the ability of axolotl decellularized ECM scaffold to improve skin wound healing in mice

Présenté par:
Walid Alariba

A été évalué par un jury composé des personnes suivantes:

Dr Antonio Nanci, président-rapporteur
Dr Stéphane Roy, directeur de recherche
Dr Jean Barbeau, membre du jury

RÉSUMÉ

Le but de notre étude visait à déterminer si les matrices ECM (extracellular matrix) préparés à partir d'un modèle vertébré (Axolotl) capables de régénérer ses tissus suite à une blessure sont plus efficaces pour stimuler les réponses régénératives chez les animaux non régénérant (par exemple les mammifères). Nous avons testé la capacité de matrice ECM axolotl à améliorer la guérison des plaies cutanées dans des souris et nous les avons comparés à une matrice disponible commercialement (échafaudage Symbios PerioDerm) pour leur efficacité à favoriser la guérison des plaies. Des lésions d'excision ont été créées sur le dos de souris et les animaux ont été regroupés dans différents groupes; a-) ECM de peau axolotl décellularisée (groupe Axolotl), b-) matrice de derme acellulaire Symbios Perioderm (groupe PerioDerm), c-) grillage en titane (groupe témoin); respectivement. Les tissus des plaies ont été récoltés à des moments précis : 7 jours et 30 jours après la blessure pour évaluer la guérison des plaies. La guérison des blessures ayant reçu les différentes matrices a été comparées entre elles en utilisant le test de transillumination et des analyses histologiques. Les résultats indiquent que la ECM de peau d'axolotl décellularisée est bien tolérée par les souris, car aucun rejet n'a été observé. Le groupe qui a reçu l'ECM de la peau axolotl décellularisé a démontré une réépithélialisation, une densité cellulaire, une teneur en collagène (avec une organisation similaire à un tissu intact) et une vascularisation (angiogenèse) élevées par rapport aux groupes PerioDerm et témoins. La présence de follicules pileux était également observé dans le groupe axolotl (qui n'est pas présent dans PerioDerm et groupes de contrôle). Sur la base de nos résultats, l'hypothèse de base semble être correcte en ce qu'une matrice ECM provenant d'un régénérateur puissant semble

favoriser la guérison plus efficacement chez les animaux normalement non régénérants. Cependant, des recherches supplémentaires devront être menées pour confirmer ces résultats.

Mots-clés: Plaie, cicatrisation, greffe, guérison cutanée, matrice extracellulaire (ECM), échafaudages, différenciation cellulaire, régénération tissulaire, biomatériaux

ABSTRACT

The aim of our study sought to determine whether ECM scaffolds prepared from a vertebrate model (Axolotl) capable of regenerating tissues following injury are more effective at stimulating regenerative responses in non-regenerating animals (e.g., mammals). We tested the ability of axolotl decellularized ECM scaffolds to improve skin wound healing in mammalian models and compare the axolotl skin ECM scaffold to a commercially available one (Symbios PerioDerm scaffold) for efficiency in promoting wound healing. Excisional lesions were created on the back of mice, and animals in different groups were treated by; a-) decellularized axolotl skin ECM (Axolotl group), b-) Symbios Perioderm acellular dermis scaffold (PerioDerm group), d-) Titanized mesh only (Control group); respectively. Wound tissues were harvested at time points: 7- and 30-days post-wounding to assess the scaffolds impact on wound healing. Wound healing was compared between the Axolotl, PerioDerm and Control groups using transillumination test and histological analyses, Results indicate that the decellularized axolotl skin ECM is well tolerated by mammalian models, as no immune rejection was observed. The axolotl group that received the decellularized Axolotl Skin ECM demonstrated high reepithelialization, cellular density, collagen content (in a porous pattern similar to intact skin), vascularization (angiogenesis) compared to PerioDerm and control groups. The presence of hair follicles was also observed in the axolotl group (which is not present in PerioDerm and control groups). Based on our results, the basic hypothesis appears to be correct in that an ECM scaffold from a strong regenerator seems to promote healing more efficiently in non-regenerating animals. However, further research should be conducted to confirm these findings.

Keywords: Wound, scarring, grafting, cutaneous wound healing, extracellular matrix (ECM), scaffolds, cell differentiation, tissue regeneration, biomaterials.

TABLE OF CONTENTS

LIST OF TABLES

Table

LIST OF FIGURES

LIST OF ABBREVIATIONS

ECM	Extracellular Matrix
©	The copyright symbol
TGF-β	Transforming Growth Factor-Beta
PDGF	Platelet-Derived Growth Factor
FGF	Fibroblast Growth Factors
HGF	Hepatocyte Growth Factor
FGF-2	Fibroblast Growth Factor-2
EGF	Epidermal Growth Factor
VEGF	Vascular Endothelial Growth Factor
IGF-1	Insulin-like Growth Factor-1
TNF-α	Tumor Necrosis Factor-Alpha
IL-6	Interleukin-6
IL-1	Interleukin-1
NA	Neutralizing Antibodies
ADM	Acellular Dermal Matrix
PBS	Phosphate Buffered Saline solution
KCL	Potassium Chloride solution
SDS	Sodium Dodecyl Sulfate solution
PCR	Polymerase Chain Reaction
rpm	Revolutions Per Minute

mL	Milliliter
µL	Microliter
M	Moles (Molarity)
Taq (NEB)	Taq Reaction Buffer (New England Biolabs)
MSX1	Msh homeobox 1 gene
HRP	Horseradish Peroxidase
TBS	Tris-buffered saline solution
CD9	Member of the Tetraspanin Protein Family
DAPI	4′,6-diamidino-2-phenylindole
EtOH	Ethyl Alcohol
H2O RO	Reverse Osmosis Water
DNA	Deoxyribonucleic acid
ALK5	Activin Receptor-like kinase 5
TβRII	Transforming Growth Factor-Beta receptor II
MAP kinase	Mitogen-Activated Protein Kinase
P38	P38 Mitogen-Activated Protein Kinase
ERK	Extracellular Signal-Regulated Kinases
JNK	C-Jun N-terminal kinases
WC	Wound Closure
NTOWA	New Tissue Over Wounded Area
VN	Vascular Network
CC	Collagen Content
CP(P)	Collagen Pattern (Porosity)
EC	Epithelial cells

EL	Epidermal Layer
BL	Basal Lamina
CT	Connective Tissue
DL	Dermal Layer
RS	Reddish Spot
PCM	*The Panniculus Carnosus Muscle*
CD	Cell Density
HF	Hair Follicle
SG	Sebaceous Gland
ML	Muscle Layer

DEDICATION

My thesis is dedicated to my beloved mother, Atiqa Jubran, and my beloved father, Mftah Alariba, who have always loved me and taught me to strive to succeed. Also, to my wife, my brothers, my sisters, and to the entire my family for supporting and encouraging me during my graduate studies

ACKNOWLEDGMENTS

First and foremost, I would like to express my heartfelt thanks to Allah Almighty for helping me to complete this project successfully. In addition, I am extremely grateful to my dearest supervisor, Dr. Stéphane Roy, without whom I never would have been able to complete my thesis. I would like to thank him for his guidance, advice, and support throughout the thesis process. Thanks to the Libyan Higher Education Ministry and the Department of Dentistry at the University of Montreal for their financial support, which enabled me to complete my master's degree. In order not to forget anyone, I would like to thank all my colleagues from the Roy lab and Nanci lab who helped me. Furthermore, I would like to thank Dr. Nanci for encouraging me to achieve my goals.

Thanks again to my mother, father, wife, brothers, sisters, and friends, for providing me with the inspiration to complete my master's degree

CHAPTER I

LITERATURE REVIEW

1.1 Introduction

1.1 Healing wounds and scarring

A wound can be described as any tissue disruption of normal anatomic structure and subsequent functional loss (1). The healing of a wound is a long and complex process during which time tissues recover from injury (2). Normally, the skin consists of two layers, the epidermis and the dermis, which act as a protective layer for the body from the environment (3). The skin serves as a physical, chemical, and bacterial barrier, so healing wounds is crucial to the body's health. Mammalian skin epidermis, as well as its appendages, such as hair follicles, sebaceous glands, and sweat glands, play crucial roles in providing dehydration protection and environmental regulation of body temperature (4). Thus, when an injury or illness causes a skin disorder there is the possibility of suffering serious physical ailments and even death.

The epidermis layer is composed of stratified keratinocytes and defined by the basal membrane (5, 6). Underneath the basal epidermal layer (which is located on top of the basement membrane) is the dermis, which is a layer of connective tissue. Essentially, the basal lamina consists of the basal cells of the epidermis and is primarily composed of type IV collagen, anchoring fibrils, and dermal microfibrils (7). The dermis provides structure and elasticity and is composed of an extracellular matrix rich in collagen and elastic fibers (8) . If the skin's protective layer is damaged, several biochemical reactions are triggered until the damage is repaired (9).

In wound healing, there are four stages: Hemostasis, Inflammation, Proliferation, and Maturation (Remodelling), which overlap in time and space (Figure 1) (10-12). First stage blood clotting (hemostasis) takes place following skin injury. During this process, the injured vessels undergo a 5- to 10-minute vasoconstricting response induced by the platelets, so as to reduce blood loss and fill the gap with a blood clot that contains cytokines and growth factors (13). Moreover, the blood

clot includes fibrin molecules, thrombospondins, vitronectin and fibronectin, forming an extracellular matrix (ECM) scaffold structure to facilitate migration of leukocytes, keratinocytes, fibroblasts, and endothelial cells. In the wound site, the platelets adhere together and release chemical signals to facilitate clotting (14). Upon activation of fibrin, a fibrin network is formed, which acts as an adhesive component that binds platelets together (15). As a result, wound openings are sealed to reduce or prevent bleeding.

Clots and surrounding wounded tissue secrete pro-inflammatory cytokines and growth factors such as transforming growth factor (TGF)-β, platelet-derived growth factor (PDGF), fibroblast growth factor (FGF), and epidermal growth factor (EGF) (16, 17). As soon as bleeding has stopped, the inflammation phase is initiated by inflammatory cells (neutrophils, macrophages, lymphocytes) invading and infiltrating the wound (18).The inflammation stage includes removing dead and damaged cells from the wound area by a process called phagocytosis, during which white blood cells engulf bacteria and debris.

In 3 days, macrophages move into the zone of injury and perform phagocytosis on pathogens and cell debris as well as secrete growth factors, chemokines, and cytokines (19). Also, white blood cells cooperate with platelets to release growth factors allowing epithelium cells to migrate and proliferate in the wound area. Both platelets and leukocytes release cytokines and growth factors, that have the ability to activate the inflammatory process (IL-1, IL-6 and TNF-α), promote collagen synthesis (FGF-2, IGF-1, TGF-β), stimulate angiogenesis (FGF-2, VEGF-A, HIF-1 , TGF-β), trigger fibroblasts to become myofibroblasts (TGF-β) and provide support for reepithelialization (EGF, FGF-2, IGF-1, TGF-β) (20).

A proliferation stage is characterized by the formation of new tissues and the secretion of factors (VEGF) by endothelial cells to help form blood vessels at the site of the wound (21). In the dermis,

fibroblasts and endothelial cells are the dominant cell types, supporting capillary growth, collagen production, and granulation tissue formation (21). Fibroblasts within the wound bed produce collagen, glycosaminoglycans, and proteoglycans, which provide the most important components to the ECM (22). During this process, collagen is synthesized in greater amounts, whereas fibroblast growth is progressively reduced, thus achieving a balance between synthesis and degradation of the ECM (22). The keratinocytes at the wound edges and the stem cells from the hair follicles and sweat glands perform the process of reepithelializing (13, 23, 24).

The final phase of wound healing is remodeling, which can take years to complete in humans following the proliferation stage and ECM synthesis. This stage is characterized by regression of many of the newly formed capillaries and remodeling of the ECM to resemble normal tissue architecture. It is also important to note that the ECM also serves as a structure for cell adhesion, which is critical for regulating and organizing cell growth, movement, and differentiation (25, 26). In the later stages, the myofibroblasts cause wound contraction and decrease scar surface (19, 27, 28).

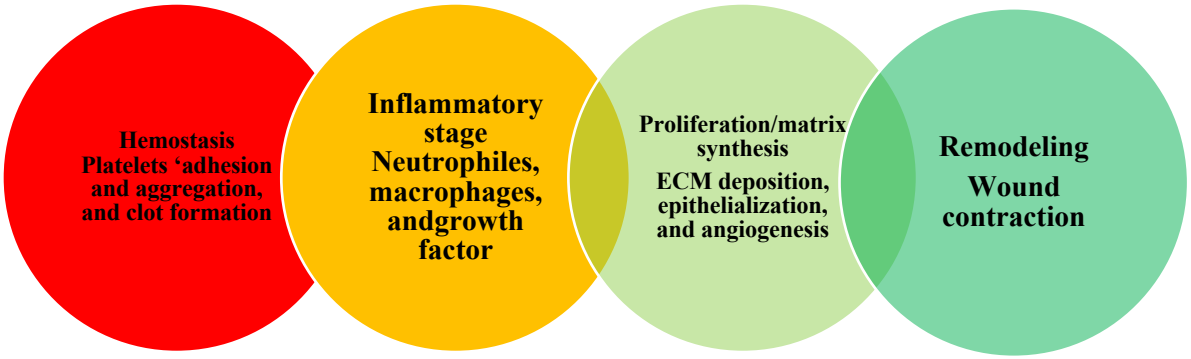

Figure 1: Healing stages

Wound healing is a delicate and complex process, so if there is any interference or failure, the wound will not be able to heal. Several factors can affect wound healing, including diabetes, vascular disease, and metabolic disorders in the elderly (29).

In the last few years, advances in cellular and molecular biology have contributed to a deeper understanding of how wound healing occurs in the body. An estimated 500,000 people in the United States undergo treatment each year for burns, the majority of which result in scarring and painful contractures requiring extensive surgical interventions (30, 31). There is a high level of social stigma and psychological distress for patients with visible scars, especially on the face (32). The scar is the body's natural way of healing and replacing lost or damaged skin. Mature cutaneous scars are composed of large amounts of collagen, of which 80-90% is type I collagen and the remainder type III collagen (33). In the case of deep wounds, scarred skin lacks dermal appendages, such as hair follicles and sebaceous glands (34-36), and wounds that are no more than two millimeters deep reepithelize and heal without scarring (37). A scarred tissue is distinguished from normal skin by the absence of rete pegs, which anchor the epidermis to the dermis beneath (38). Basement membranes of the epidermis that develop over scar tissue are flatter than normal, since they do not contain the rete pegs that penetrate into the dermis normally (33). Changes within the ECM as well as in the epithelium of the skin are also believed to contribute to excessive scarring (39, 40).

In mammals, fetal tissues are capable of healing without scarring. Scarless wound healing is discontinued in humans after approximately 24 weeks of gestation, whereas it ceases in mice on day 18.5 (29, 41, 42). Several research studies have demonstrated that the fetus heals wounds more rapidly and more efficiently, and that the resulting tissue regenerates completely. It is interesting to note that even dermal appendages like sebaceous glands and hair follicles can heal after fetal

injury (43). Studies have indicated that scarless wound healing occurs in fetal tissue due to differences in the extracellular matrix (ECM), inflammation, cellular mediators, gene expression, and stem cell function (44, 45). It may be possible to use fetal wound healing as a model of wound healing in mammals to obtain the best response in adult wounds. Interestingly, some vertebrates such as urodele amphibians (newts and axolotls) have the unique ability to regenerate tissues and heal wounds without scarring over their entire life span (46-49). Thus, wound healing in a newt and axolotl may be used as a model for reducing wound scarring and complications in mammals.

1.2 Treatment of wounds and minimize scarring

It is expected that the wound care products market will reach $15-22 billion by 2024 (50). According to estimates, there are over 2% of the American population who are thought to suffer from chronic wounds (51). As a result of trauma or surgery, more than 100 million people suffer from scarring each year, resulting in pathologies ranging from thin surgical scars to chronic non-healing wounds (52, 53). There are several surgical and pharmaceutical options available for treating and preventing scarring, though none of them is sufficient to prevent scarring from occurring, particularly in patients with severely damaged skin. In chemical peels, chemicals are used to exfoliate the skin in a controlled manner, leading to a reduction of superficial scarring (54). The use of collagen filler injections can be used to elevate atrophic scars to the same level as the surrounding skin (55). A laser is commonly used to remove hypertrophic scars, such as keloids, as well as to improve the appearance of burn scars (56). In some cases, superficial radiotherapy can be used to prevent recurrence of severe scarring and hypertrophic scarring (57). Additionally, intra-lesional injections of corticosteroids are commonly prescribed to treat pathological scarring (58).

There are several physical, medical, and surgical methods available for treating or at the very least reduce scarring. Also, many attempts have been made to test the efficacy of novel agents for treating scarring and other fibrotic conditions in humans, but the results have been disappointing. The injection of neutralizing antibodies (NA) to transforming growth factor-β (TGF-β) at the edge of the wound has been tested on mice to promote wound healing (59). The wounds treated with NA had a more normal, regenerative pattern of dermal architecture, as demonstrated by the orientation of collagen fibers (60), than did controls, which had many abnormally oriented collagen fibers within the scar (59). The extracellular matrix (ECM) graft can promote wound healing by stimulating cell migration and proliferation within the ECM, especially if it contains growth factors. Several functions of the ECM are known, including organogenesis, tissue repair, maintenance of cellular organization in adults, and the prevention of tumor invasion (61).In the extracellular matrix, specific attachment sequences are recognized by receptors known as integrins on the cell surface (62). ECMs play an important role in wound healing as well as acting as a reservoir and modulator of cytokines and growth factors (63, 64). As scaffolds also serve as a bridge between the border of the wound to allow cells to migrate and proliferate, thus they are potentially able to accelerate wound healing while minimizing scarring (Figure 2).

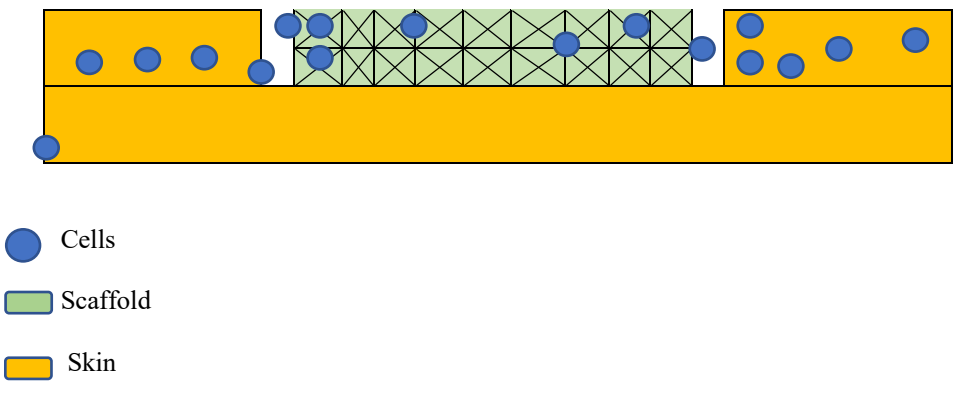

Figure 2: Migration of cells within the scaffold

A scaffold can be classified as either a natural scaffold (derived from organic skin living cells) or a synthetic scaffold (derived from biomaterials). Many synthetic scaffolds can promote wound healing, especially those that contain growth factors that stimulate the proliferation of cells within the scaffold. Various biomaterials are used to treat acute and chronic wounds. However, each has its own advantages and disadvantages (65-67).

A natural scaffold may be a better alternative to synthetic scaffold since it contains natural growth factors, some of which are yet unknown, and it is characterized by a three-dimensional structure that facilitates cell proliferation and distribution inside the scaffold rapidly. An acellular dermal matrix (ADM) is a natural scaffold that may function as protective barriers, a scaffold on which cells can migrate, and to signal cells in a manner that promotes angiogenesis and granulation tissue ingrowth (68, 69).

1.2 Regenerating wounds in some animals

Natural science, especially zoology and embryology, has been fascinated by some animals' ability to regenerate parts of their bodies following amputation or injury, for hundreds of years. While complex tissue regeneration is not observed in the mammalian body, it is much more common in amphibians. The urodele amphibians (also known as salamanders) are one group of tetrapod vertebrates that have developed the ability to regenerate complex tissues throughout their lifetimes. Research has often been carried out using urodeles such as axolotls and newts to study regeneration, however, there have also been studies performed using the Japanese fired belly newt. In addition, the European ribbed newt, is also capable of regeneration. In short, it has been shown that there is no better regenerator among all the vertebrates than urodeles. It is known that urodeles are capable of regenerating entire limbs after having been amputated (48, 70). Additionally,

urodeles have the ability to regenerate a variety of tissues and organs, including the spinal cord, the heart's apex, a portion of the forebrain, and certain internal organs after injury (71, 72).

The axolotl skin can regenerate completely after excision of the epidermis, dermis, and muscles (73, 74). In amphibians, skin can regenerate or heal on its own without the formation of scar tissue (73, 75, 76). In addition, anurans (frogs) are capable of completely regrowing a limb after amputation, but adults do not possess this capability (77). Moreover, research has revealed that the skin of amphibians (frogs and salamanders) contains peptides and proteins that promote wound healing in mammals (78, 79). There is also a growing interest in using frog skin as a biological dressing for severe burns in some countries with positive results (reduced infection and faster healing) (80). In the first trimester of gestation, the skin of mammals can heal without scarring. After that, the skin wound healing turns to scarring (81, 82). Spiny mice of Africa are the only mammals known to be able to regenerate damaged tissue (83). Furthermore, it is not known whether *the panniculus carnosus* of spiny mice is fully recovered, which is a structure essential for wound contraction in animals with loose skin, because it was not visible either in the healed skin or in the cartilage with the ear holes (76). As previously stated, animal models that possess the ability to regenerate tissues can be useful in determining which pathways in humans must be inhibited or stimulated to promote wound healing. Animals such as axolotls, which are known to have the capacity to regenerate fully, will likely play a significant role in helping humans achieve scarless wound healing.

1.3 Rationale

As a result of mammals' inability to regenerate wounds instead of forming scar tissue, a variety of technical approaches have been developed to aid in the direction of various types of wounds

towards regeneration. The development of biomaterials to facilitate wound healing has been the subject of much attention and funding for many decades. Additionally, biomaterials have been tested as potential medical devices (84). Moreover, the term "tissue engineering" was introduced in 1988 and described as "*the application of the principles and methods of engineering and life sciences toward the fundamental understanding of structure-function relationships in normal and pathological mammalian tissue and the development of biological substitutes to restore, maintain, or improve tissue function*" (85). Over the past decade, however, it has become evident that one of the most promising biomaterials can be found in the extracellular matrix of the various animals and organs themselves (86, 87). Moreover, the ECM is rich in growth factors, hence it can affect the migration of cells into the wound bed as well as stimulate wound healing and regeneration (85, 88). It may be possible or expected that biomaterials are not as effective as ECMs for wound healing (89). This explains why a variety of scaffolds derived from different types of animals have been developed for use in humans (90). The acellular dermis (from cadavers), the pig bladder ECM scaffolds, and the fetal bovine dermis have all been used or tested as grafts for wound healing in humans (91). Moreover, there are also biomaterials derived from crustacean shells (chitosan), which are being tested for regenerative functions (92). In the ECM, growth factors are naturally stored (e.g., FGF, TGF-β, VEGF, PDGF and HGF) and play an important role in wound healing and regeneration (85, 93).

However, researchers have not been able to pinpoint which growth factors or combinations of macromolecules (collagen, fibronectin, tenascin, hyaluronic acid, glycosaminoglycans) are optimal to stimulate regenerative responses. The ECM of salamanders consists of two important components, fibronectin and tenascin, which mediate cell migration and proliferation in the regenerative process (75, 94). Thus, the purpose of this thesis is to test the hypothesis that ECM

scaffolds derived from axolotl skin may promote wound healing in non-regenerating organisms (e.g., mammals). Moreover, the purpose of this thesis is to examine if Symbios PerioDerm scaffold may also promote wound healing and to compare this scaffold to ECM scaffold derived from axolotl skin in order to determine which scaffold is more effective at improving wound healing. Symbios PerioDerm scaffolds are acellular dermal allografts that are designed to augment or replace damaged or inadequate tissue during the repair, reinforcement, or replacement of soft tissue defects. Moreover, Symbios PerioDerm scaffolds provide treatment of gingival recession as soft tissue thickness is increased in the implant socket and prosthodontic management (95, 96). This thesis is innovative in that it considers both fundamental questions about the role of the extracellular matrix in promoting healing as well as the possibility of developing new biomaterials to improve human health after suffering burns or injuries that result in scarring.

CHAPTER II

METHODOLOGY

2.1 Preparation axolotl skin scaffold (ECM)

This experiment was performed according to the guidelines set by the Université de Montréal Animal Care Committee. Axolotls were purchased from Ambystoma Genetic Stock Center (Lexington, KY) and were being cared for according to the instructions given by Lévesque et al (97). An axolotl (female, white, 3 years old), was anesthetized by placing it in a container filled with 0.2% MS222 for 20 minutes. Afterward, the axolotl was euthanized by decapitation, the skin from its back was carefully removed and the dermis (including muscles and fat) was carefully cleaned with a scalpel. After washing the skin with 1X PBS, the skin is decellularized in order to reduce the possibility of rejection by the immune system when the skin is grafted on mice.

The decellularization process was carried out with three cycles of freezing (-80°) and thawing (37°) to destroy the cellular membrane and nuclei without damaging the collagen of the extracellular matrix (Table 1). Then it was rinsed once in dH2O/300 ml with shaking 200rpm, 1h at room temperature, and then once in 1X PBS/300ml with shaking 200rpm, 5h at room temperature, in order to eliminate the cellular debris.

Afterwards, it was rinsed 1X with 1M KCL/300ml with shaking 200rpm for 24 hours at 37 degrees Celsius, followed by rinsing with dH2O/300 ml with shaking 200rpm. Afterwards, it was placed in 1% SDS/300ml by shaking 200rpm for 48 hours at 37 degrees Celsius (changing solution after 24 hours). It was then rinsed with 3X in dH2O water, 200rpm, for 1 hour at room temperature. Next, it was placed in dH2O containing detergent (1% TritonX-100)/300ml with shaking 200rpm, 24h at 37°C, and it was then rinsed in 3X in dH2O/300ml with shaking 200rpm, 1h at room temperature.

Scaffold was rinsed in 1X PBS/300ml with shaking 200rpm for 5 hours at room temperature, and then in 1X dH2O/300ml with shaking 200rpm for 1h at room temperature. Then it is lyophilized and stored at -80 until it is ready to use.

	The decellularization process
1	Three cycles of freezing (-80°) and thawing (37°)
2	Rinsed in 1X dH2O/300 ml with shaking 200rpm, 1h at room temperature
3	Rinsed in 1X PBS/300ml with shaking 200rpm, 5h at room temperature
4	Treat with 1X 1M KCL/300ml with shaking 200rpm for 24 hours at 37 degrees Celsius
5	Rinsed in 1X dH2O/300 ml with shaking 200rpm
6	Treat with 1% SDS/300ml by shaking 200rpm for 48 hours at 37 degrees Celsius
7	Rinsed in 3X in dH2O, 200rpm, for 1 hour at room temperature
8	Treat with detergent 1% TritonX-100/300ml with shaking 200rpm, 24h at 37°C
9	Rinsed in 3X dH2O/300ml with shaking 200rpm, 1h at room temperature.
10	Rinsed in 1X PBS/300ml with shaking 200rpm for 5 hours at room temperature
11	Rinsed in1X dH2O/300ml with shaking 200rpm for 1 hour at room temperature
12	Lyophilized and stored at -80 until it is ready to use

Protocol for decellularizing axolotl skin according to Roy's lab (Table 1)

2.2 DNA isolation and RT-PCR

Polymerase chain reaction (PCR) was conducted to determine whether DNA fragments (highly inflammatory) were present in decellularized axolotl skin (ECM). DNA was extracted from axolotl decellularized ECM and intact skin (to serve as a positive control). One small piece of decellularized and intact axolotl skin (ECM) was frozen with liquid nitrogen and broken up with a mortar and pestle. Each of them was collected as powder and placed in a centrifuge tube with 2ml of 1X PBS. Then, they were homogenized using high-shear homogenizers. The PCR reactions were performed using 1X standard Taq NEB reaction buffer. 40 cycles of PCR amplification were

performed using the following protocol 60° for primers forward; MSX1 1 IN FX3, and reverse primers; MSX 1 R877. Samples of PCR products (7uL decellularized axolotl skin, 7uL intact axolotl skin mix, and 7uL water blank) were added to 1uL Orange G stain. Then, 0.7uL of 1KB Ladder was added to 1uL of orange G stain. After that, all samples were loaded and resolved in 1% agarose gels (30mL of H_2O NANO, 600µL of TAE 50X, 0.3 g Agarose powder)

2.3 Indirect Immunofluorescence

To evaluate the integrity of the decellularized axolotl skin ECM from any damage, indirect immunofluorescence to detect collagen-IV was used (98). Firstly, the slides were deparaffinized in three separate baths of xylenes for five minutes each. Following this, slides were rehydrated in a series of 100%, 95%, 70% alcohol for 5 minutes each and then placed in water followed by a heat-induced epitope retrieval (20 min at 95°C) in 0.1 M citrate at pH 6.0. The slides were then blocked in TBS-T with 2% BSA for 15 minutes.

The primary antibody (anti-col-IV, ab6586, 1/500) was diluted in blocking solution and incubated on slides overnight at 4°C. Then, all slides were rinsed with (PBS 1X) three times for five minutes. The secondary HRP coupled antibody (anti-rabbit HRP, cat# 170-6515, Biorad, 1/400) was diluted in blocking solution just as for anti-collagen-VI and incubated on slides for 45 minutes at room temperature. After this, all slides were rinsed with (PBS 1X) three times for five minutes. Tyramide (Biotium, San Francisco Bay, CA, cat# 92175) was diluted in 1X TBS with 0.0015% H2O2 to an active concentration of 11.6µM then incubated on slides at room temperature for 8 minutes. Following this, all slides were rinsed with (PBS 1X) three times for five minutes. Afterwards, slides were mounted with ProLong® Gold antifade reagent and observed with a Zeiss Axio Imager M2 Optical Microscope (Zeiss, Munich, Germany).

2.4 Materials and surgical instruments

The scaffolds (Symbios PerioDerm Acellular Dermis, 2 cm x 4 cm) were purchased from Dentsply Sirona, Mississauga, ON, Canada. Decellularized Axolotl Skin scaffolds and PerioDerm Acellular Tissue Scaffolds (figure 3A), and Titanized Mesh (figure 3B) were prepared by cutting them in a circular pattern (size 8mm for Axolotl and Prioderm scaffolds and 10mm for Titanized Mesh) which were performed by punch biopsy (size 8-10mm). Titanized mesh was used to prevent contraction of the panniculus carnosus in the wound area. Tegaderm (Nexcare 3M) Nexcare wound dressings, and callus cushions, for protecting the wound area from infection or any damage during mice activity, were purchased from Pharmaprix and PJC Jean Coutu in Montreal, Canada (figure 4). The suture needles (Ethicon 5-0 x 18" Ethilon® Nylon Clear Sutures with P-3 Needle - 12/Box), scissors, and sterile punch biopsy (Acuderm P550 ACU-Punch Biopsy Punches (8-10) mm, Box of 50), inhalational anesthesia (isoflurane), normal sterile saline, a needle holder, and Addison forceps (figure 5).

2.5 Animal Maintenance and Excisional Wounding steps

The immune-competent mice (CD9 from Charles River, Montreal Canada) were purchased, and housed at the animal care facility at Montreal University. A total of 18 male mice (weighing 35-45g and aged 2-3 months) were selected at random and divided into three groups of three mice each. All mice were housed in cages with free access to standard pellet food and water, under the following conditions: at room temperature (around 24°C), with 12 hours of darkness followed by 12 hours of light.

Symbios PerioDerm Acellular Dermis

A

Titanized Mesh

B

Figure 3 Materials and surgical instruments

Wound dressing

Callus cushions

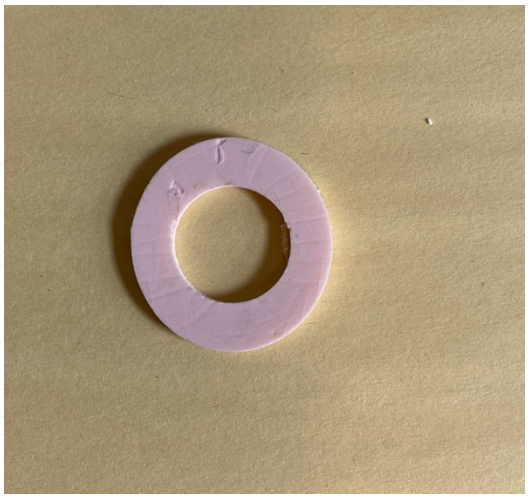

Tegraderm (Nexcare 3M)

Figure 4 Materials and surgical instruments

Suture needles (Nylon Suture)

Sterile punch biopsy 8mm

Sterile punch biopsy 10mm

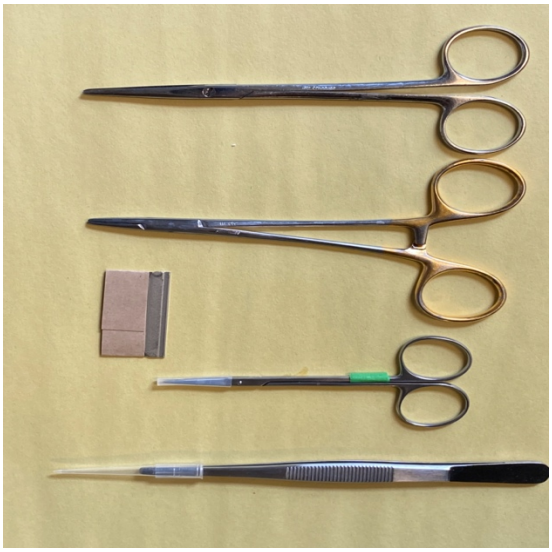

Surgical tools

Figure 5 Materials and surgical instruments

The mice were administered 0.05-0.1 mg/kg of buprenorphine slow release (done by the veterinary services of the Universté de Montréal) prior to anesthesia in order to reduce postoperative pain, and then inhalation of isoflurane was used as a general anesthetic. The backs of anesthetized mice (n = 18) were shaved, and the area of the wound was washed with normal sterile buffer to remove any contamination that might lead to infection. Two full thickness skin excisions were made with a 10 mm diameter punch biopsy tool (Figure 6).

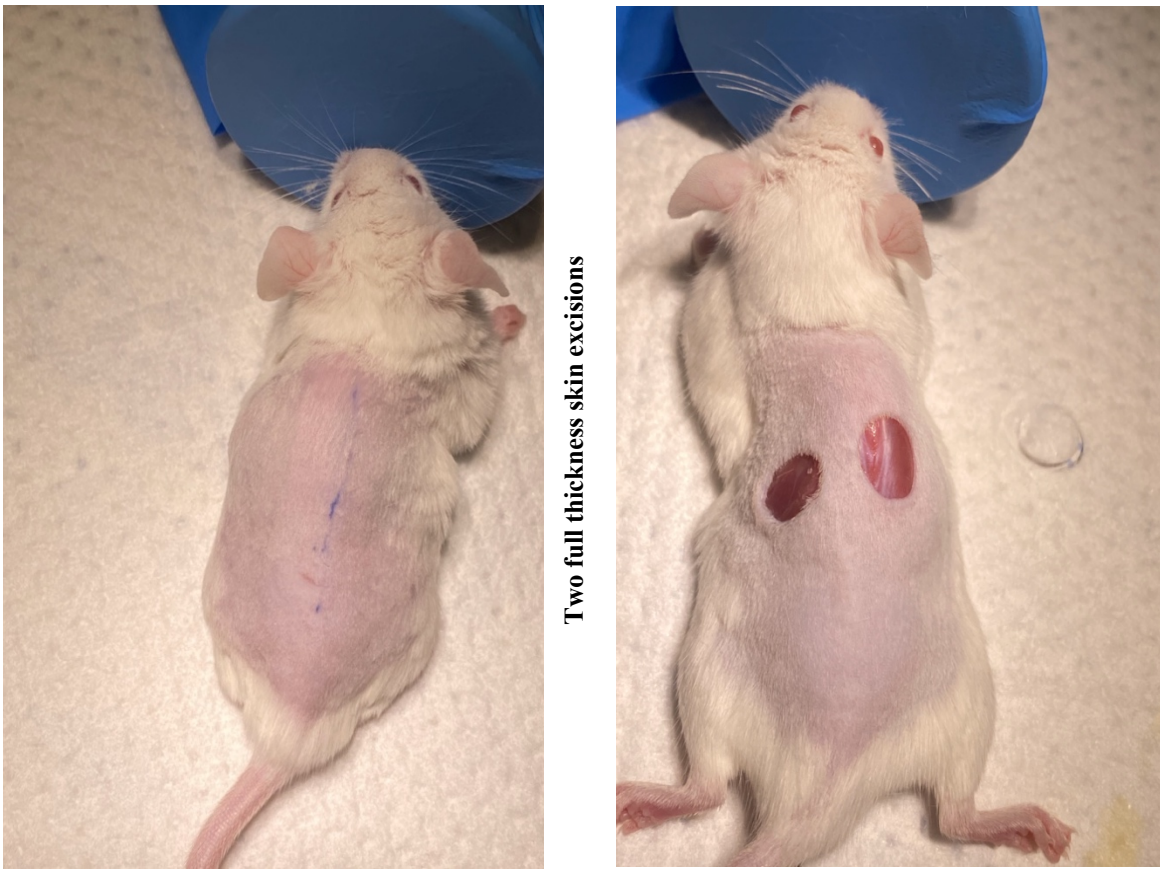

Figure 6 Excisional Wounding steps

After wounding, Titanized mesh is placed directly on the wound bed for the control group, and it is sutured with eight stitches. In the Axolotl and Perioderm groups, Titanized mesh and scaffolds (axolotl and Perioderm) were placed and then stitched together with eight stitches each (figure 7). Photographs were taken on day 0 with an iPhone 11 Pro, then Callus cushions were placed and sutured with tie stitches around the wound area. Then it was covered with Tegaderm (Nexcare 3M), followed by a non-sticky dressing (figure 8A, B, C, D). All mice were injected subcutaneously with normal sterile saline (0.5 ml) in order to prevent dehydration. The following groups have been assigned:

Axolotl Group Axolotl (n=6): The first experiment was conducted using three decellularized axolotl skin ECM scaffolds in which they were grafted on 3 mice for the period of time 7 days, and the second experiment was performed using three decellularized axolotl skin ECM scaffolds in which they were grafted on 3 mice for the period of time 30 days.

Perioderm Group (n=6): The first experiment was carried out using three Symbios Perioderm acellular dermis scaffolds in which they were grafted on 3 mice for the period of time 7 days and for the second experiment was performed using three Symbios Perioderm acellular dermis scaffolds in which they were grafted on 3 mice for the period of time 30 days.

Control Group (n=6): The first experiment was carried out using three titanized meshes in which they were grafted on 3 mice for the period of time 7 days, and the second experiment was performed using three titanized meshes in which they were grafted on 3 mice for the period of time 30 days. The animal experimentation has been approved by the animal care and ethics committee of Université de Montréal, which is recognized by the Canadian Council for Animal Care.

The mice were euthanized by Carbon dioxide exposure and decapitated on day 7 and day 30, and the wound closure rate was determined by taking photographs of each wound using an iPhone 11 Pro on days 0, 7, 22 and 30, in the first and second experiments.

2.6 Transillumination Test

Transillumination (shining light) was used to detect the presence of vascular networks. On days 7 and 30, the skin containing the whole wound area was removed from mice in all groups. Then, they were stretched on a light source and photographed with an iPhone 11 Pro.

2.7 Histological analysis

The slides were stained with DAPI staining, which stains DNA, in order to determine whether the decellularized Axolotl Skin ECM had completely decellularized. Additionally, the slides were stained with Sirius Red and Hematoxylin and Eosin to assess the collagen content and presence of cells in the granulation tissues of Axolotl, Perioderm, and control groups.

2.7.1 Staining with DAPI

This method was used to determine if any cells were left in the ECM of decellularized axolotl skin. The slides were deparaffinized in 3 baths of xylenes for 5 minutes each and rehydrated in successive concentrations of 100%, 95%, 70%, and 50% alcohol. All slides were then distilled in water for 5 minutes and mounted with ProLong® Gold antifade reagent containing DAPI (4′,6′-Diamidino-2-phenylindole). Afterward, they were visualized using a Zeiss Axio Imager M2 Optical Microscope (Zeiss, Munich, Germany).

2.7.2 Staining with Sirius red

It is important to detect the collagen pattern in order to determine if they are normal collagen patterns or abnormal collagen patterns (scarring). The samples were fixed in 4% paraformaldehyde in 0.7× PBS at 4°C overnight. Afterwards, tissues were rinsed thoroughly with 1× PBS and embedded in paraffin. Before staining, sections (10 μm in thickness) were deparaffinised through three baths of xylene for 5 min each. Slides were then rehydrated in a graded series of 100, 90, 70, and 50% ethanol, and then in distilled water for five minutes.

All slides were then soaked in Weigert's Hematoxylin for 10 minutes. Then, rinsed three times with distilled water (H2O RO) for ten minutes. Next, the slides were soaked in Sirius Red 0.1% m/v (Direct Red 80 (Alfa Aesar, B21693) in a saturated solution of Picric Acid) for 1 hour. Afterward, slides were washed in acetic acid 0.5% v/v for 2X5min followed by rapid dehydration in 90% EtOH, 100% EtOH, and 100% Xylene for 2X5min each. After that, Permount (Fisher scientific, Ottawa, Ontario, Canada) was used to mount the slides. Polarized light was used to visualize collagen by a Zeiss Axio Imager M2 Optical Microscope (Zeiss, Munich, Germany).

2.7.3 Staining with Hemoxylin & Eosin

This method is useful in detecting cells, appendages of dermis, and different layers of skin in a wound area, which can then be compared to that of a normal skin layer. The slides were deparaffinised and rehydrated as described above for Sirius red staining. Following rehydration, the slides were subsequently stained in Mayer’s hematoxylin (Dako Cytomation, S3309) for 75 sec, thoroughly rinsed in water, put in 0.08% NH_4OH for 20 sec, in 80% ethanol for 1 min, in Eosin for 30 sec and rinsed in 80% ethanol for 30 sec. Then, slides were dehydrated in 95% ethanol two times for 1 min, 100% twice for 1 minute and two times in xylene for 1 minute. The mounting

was performed with Permount^{TM} Mounting medium (Fisher Scientific, Sp15-100). Zeiss Axio Imager M2 Optical Microscope (Zeiss, Munich, Germany) was used to visualize the slides.

2.8 Semi-quantitative analysis

The microscopic scale was used for histological staining with Hematoxylin & Eosin and Sirius Red. A macroscopic scale was also used for wound closure and transillumination tests. The wound closure (tissue closure), the percentage of new tissue over the wounded area, presence of vascular network and collagen content (density), collagen pattern (porosity or mesh like structure), amount of epithelial cells, recovery of the epidermis over the wounds (Epithelial Layer), presence of the basal lamina, connective tissue (Dermal Layer), *the panniculus carnosus muscle* (Muscle Layer), cell density in wound tissue sections, presence of reddish spots and dermal appendages (hair follicles and sebaceous gland) were assessed and scored in a semi-quantitative analysis. The scoring is compared to Control group was labelled as follows: none= –, low= +, moderate= ++, high= +++.

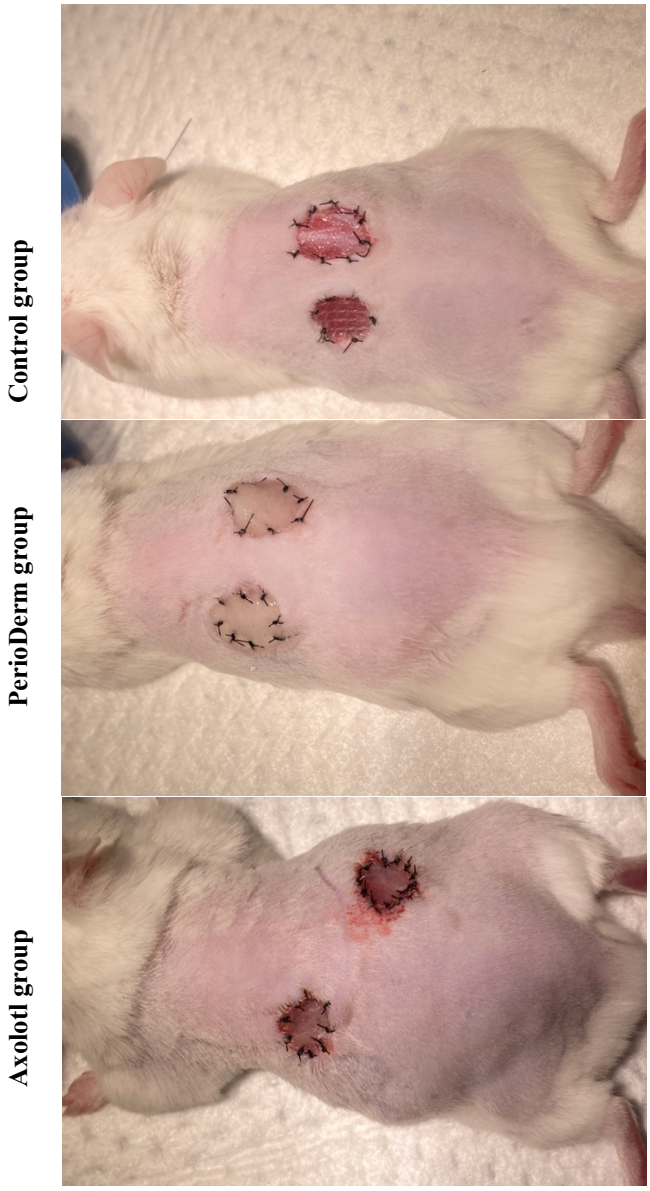

Figure 7 Excisional Wounding steps

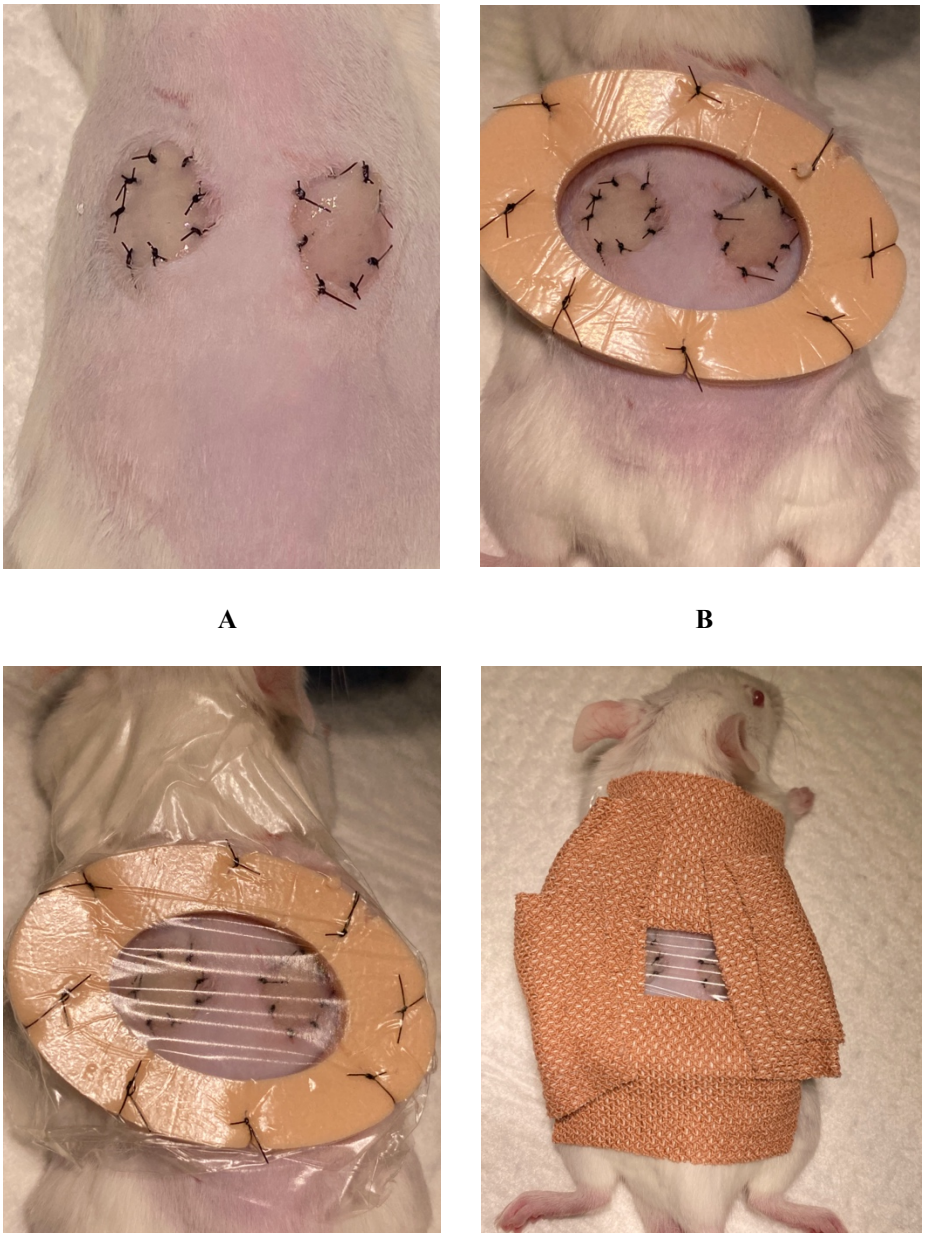

A **B**

C **D**

Figure 8 Wound dressing steps

CHAPTER III

RESULTS

3.1 Assessment the Decellularized Axolotl Skin ECM

The methods of DAPI staining, which stains DNA, and PCR have been used to verify that cells were removed from decellularized axolotl skin in order to avoid triggering an immune response against the xenograph. The decellularized axolotl skin ECM has also been examined using Sirius red and indirect immunofluorescent staining of collagen IV to determine whether any damage had occurred following the decellularization procedure.

3.1.1 DAPI staining

As a result of DAPI staining, the decellularized axolotl skin ECM did not stain for nuclei in comparison to those of normal axolotl skin (Figure 9). The negative staining of nuclei by DAPI (Figures 9A, B) indicated successful removal of cells in Decellularized Axolotl Skin ECMs, whereas intact axolotl skin (Control) containing cells showed positive nuclear staining by DAPI. (Figures 9C, D).

3.1.2 Collagen staining with Sirius red

Sirius red staining was used to determine whether or not collagen content and orientation of fibers within the decellularized Axolotl Skin ECM had been damaged. Staining with Sirius Red revealed collagen fibers (red) in the Decellularized Axolotl Skin ECM (Figures 10A and 11A) and in the intact axolotl skin (Figures 10B and 11B). The red collagen fiber indicates collagen is still readily apparent in the decellularized axolotl skin. Thus, the collagenous matrix structure and collagen organization of the decellularized axolotl skin ECM were likely maintained after decellularization (Figures 10A, 11A).

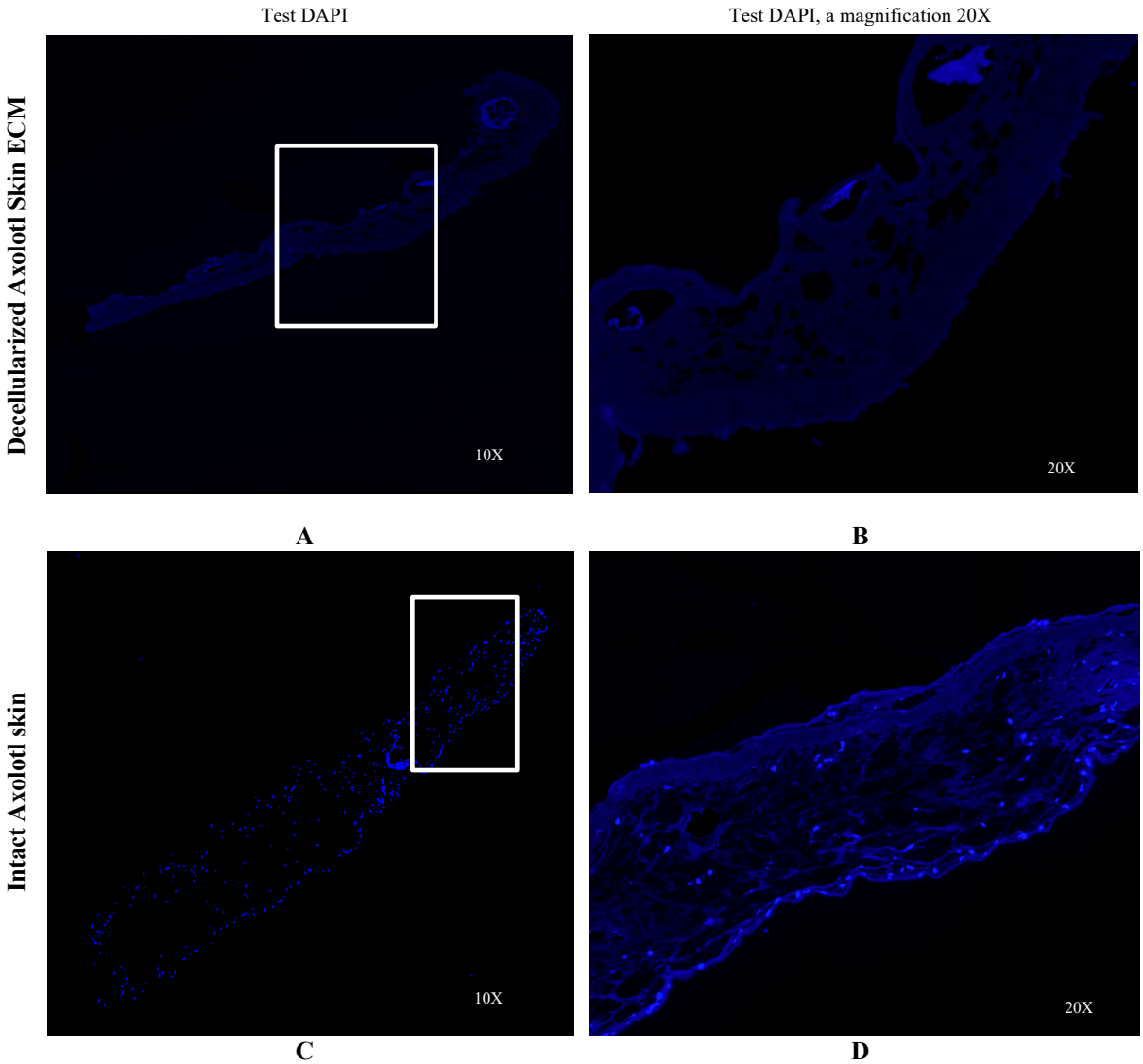

Figure 9 DAPI staining of the decellularized axolotl skin ECM. Axolotl decellularized skin (Figure 9A, B) shows negative staining for nuclear DNA, indicating the absence of cells, while intact skin (Figure 9C, D) shows positive nuclear DNA staining, indicating the presence of cells.

In the Polarization field (Sirius red staining)

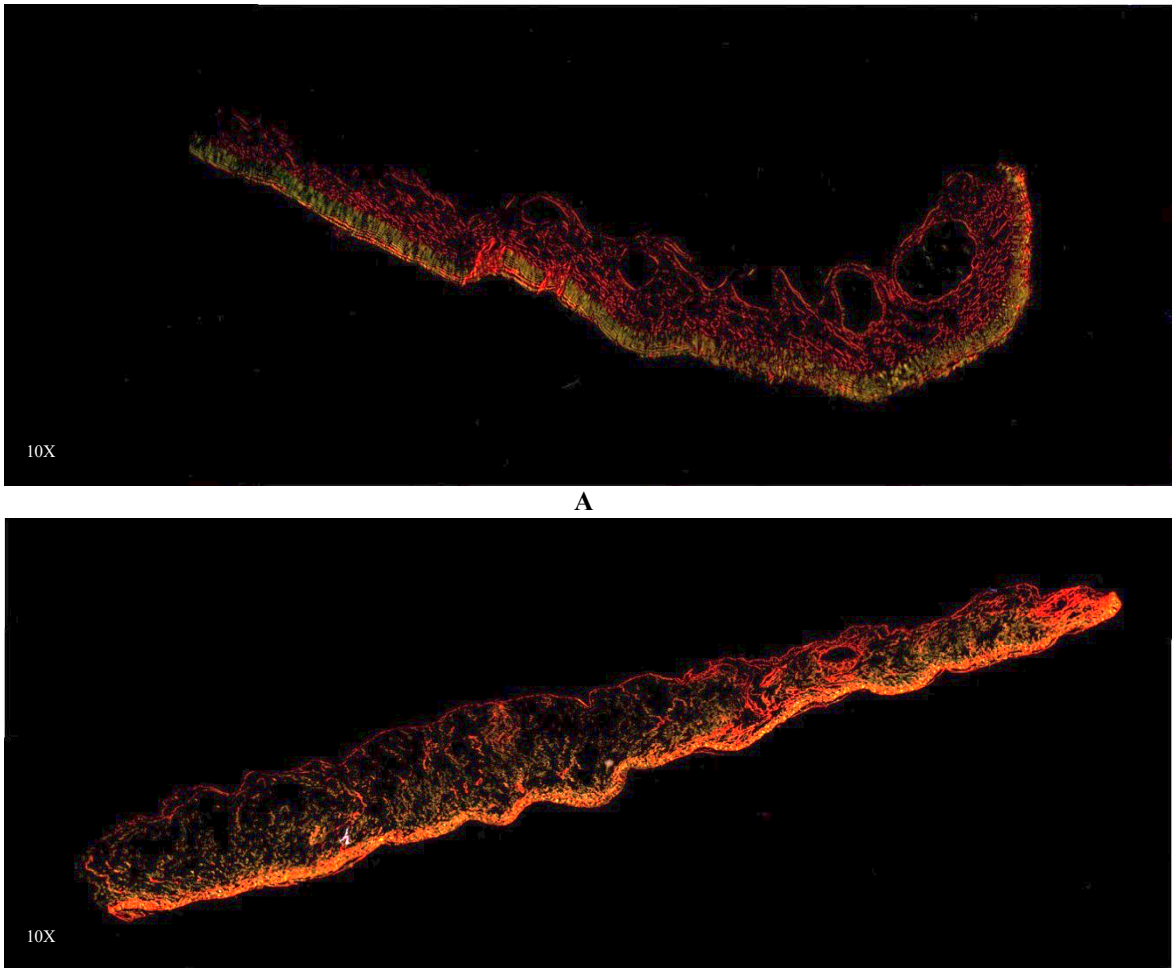

Figure 10 Sirius red of the decellularized axolotl skin ECM in the Polarization field, Sirius red stain imaging, a magnification 10X, revealed general maintaining collagen in the decellularized axolotl Skin ECM (A) and intact axolotl skin (B).

In the White field (Sirius red staining)

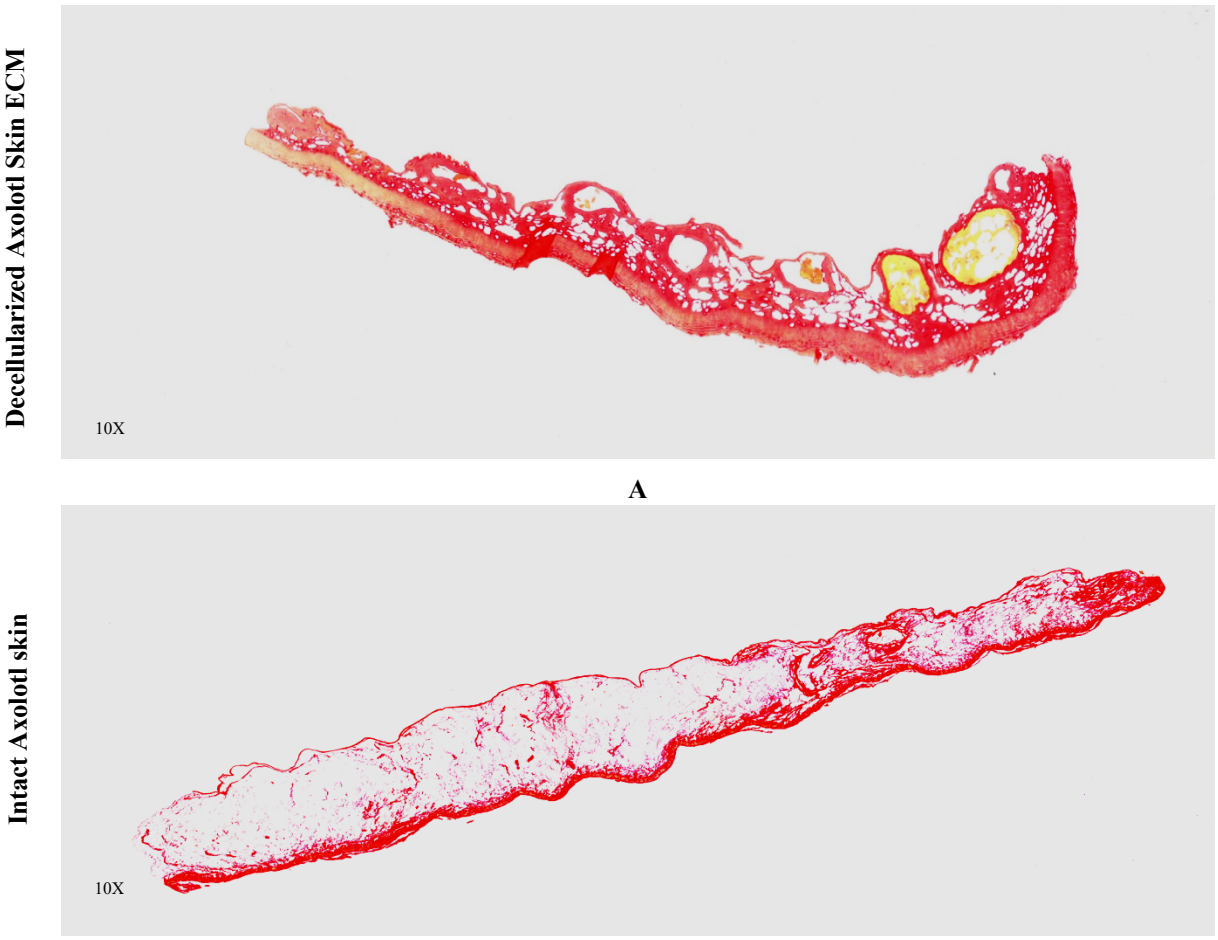

Figure 11 Sirius red of the decellularized axolotl skin ECM in the white light, Sirius red stain imaging, a magnification 10X, demonstrated the presence of general maintaining collagen of Decellularized Axolotl Skin ECM (A), and intact axolotl skin (B).

3.1.3 Indirect immunofluorescent localization of collagen IV

The basement membrane glycoproteins are normally associated with collagen type IV. Therefore, indirect immunofluorescence localization of collagen IV was carried out in order to determine if damage had occurred to the decellularized axolotl skin ECM. The collagen IV fibers were visualized by immunofluorescence in both decellularized axolotl skin ECM (Figure 12A) and in intact axolotl skin (Figure 12B). The collagen IV fibers were well preserved after decellularization in comparison to intact axolotl skin. Thus, decellularization did not change the distribution of collagen IV that is present in normal axolotl skin tissue.

3.1.4 Detection of genomic DNA in decellularized axolotl skin

A fragment of genomic DNA of 500 bb of the MSX1 gene intron (1 intron in the axolotl MSX1 gene) was amplified using PCR to determine whether any genomic DNA was still present in the decellularized axolotl skin. Remaining genetic materials, such as DNA fragments, are capable of inducing an immunogenic rejection response. In order to assess for the presence of DNA fragments and to avoid triggering an immune response against the xenograph, the presence of residual genomic DNA after decellularization was measured using PCR. There was a significant difference in DNA content between Decellularized Axolotl Skin ECM and intact Axolotl skin. Neither Decellularized Axolotl Skin ECM nor water blank (negative control) showed any DNA amplification, however intact skin displayed an intense amplified band at 500 kb (expected size of the amplicon) (Figure 13). Thus, cells and genomic DNA were successfully removed from Decellularized Axolotl Skin ECM as there was no genomic DNA detected.

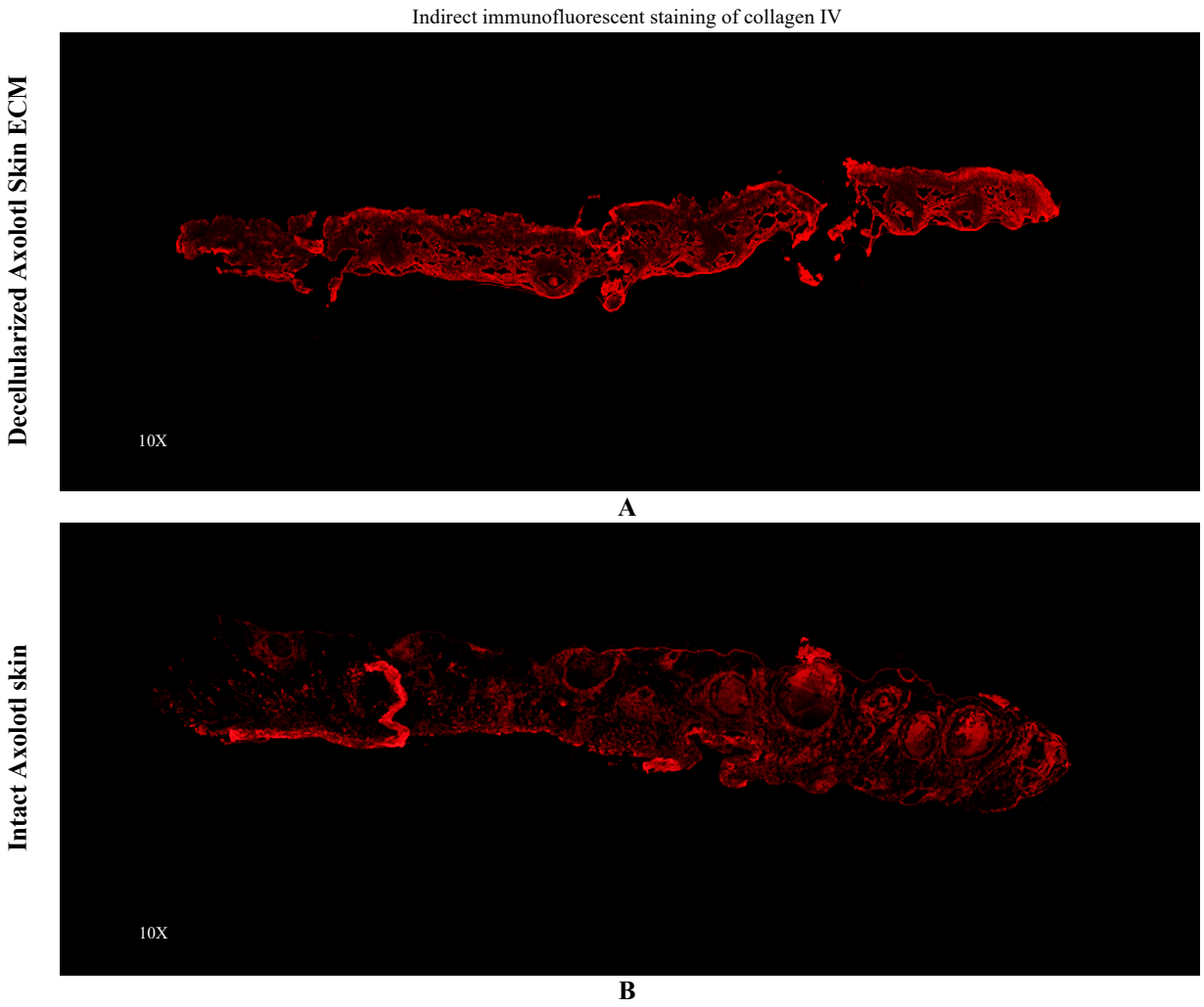

Figure 12 Indirect immunofluorescent staining of collagen IV, an image of indirect immunofluorescent, a magnification 10X, staining showing the general histoarchitecture of collagen IV (red indicates collagen IV presence) in Decellularized Axolotl Skin ECM (A) was preserved after decellularization when compared to intact axolotl skin(B).

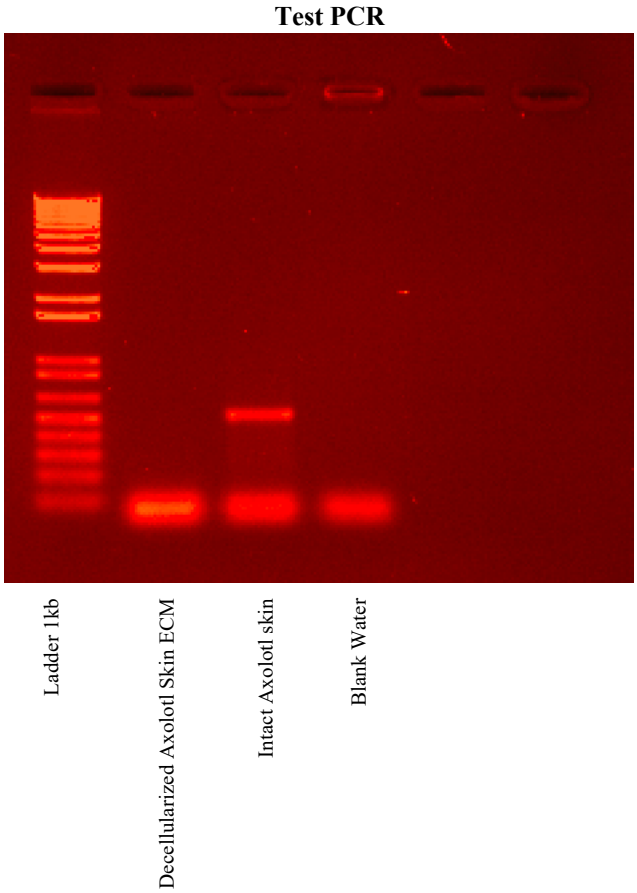

Figure 13 PCR amplification of genomic DNA (intron of axolotl MSX1 gene). The PCR results of intact Axolotl skin on gel electrophoresis showed a large band of DNA at >500 bp, but the Decellularized Axolotl Skin ECM and blank water showed no DNA band.

3.2 An assessment of grafts (Axolotl, PerioDerm, and Control groups) in mice after 7 and 30 days.

Both seven-day and thirty-day experiments were carried out using decellularized Axolotl Skin ECM (Axolotl group), Symbios PerioDerm acellular dermis scaffolds (Perioderm group), and Titanized meshes only (Control group). The grafts were placed on the backs of mice for 7 and 30 days. We assessed the Axolotl, Perioderm, and Control grafts at 7 and 30 days through wound closure, transilluminating test, and histological analysis (staining Sirius red with Eosin & Hematoxylin Sirius red).

3.2.1 Wound closure

The wounds (8 mm excisional) were photographed immediately following surgery (0 day) and post-surgery (7, 21 and 30 days) in both seven-day and thirty-day experiments (Figures 14, 15) There were no differences in the percentage of wound closure between Axolotl, Perioderm, and Control groups at 7 days in both the seven-day and thirty-day experimental animals, but at 21 days and 30 days in the thirty-day experimental groups, there were differences in the size of tissue closure between Axolotl, PerioDerm, and Control groups (Figures 14, 15) (Table 2). After 21 days, the tissue closure in the Control group was ++, while tissue closure was + in the Perioderm and Axolotl groups. However, tissue closure was +++ in all groups (Axolotl, Perioderm, Control) after 30 days.

Axolotl, PerioDerm, and Control groups also showed no differences in new tissue over the wounded area at 7 days in both seven-day and thirty-day experiments, but the presence of new tissue over the wounded area showed differences on day 21 and day 30 in thirty-day experiments (Figures 14, 15) (Figures 22A, B, C, 24A, B, C) (Table 2). Following 21 days and 30 days, the presence of new tissue over the wound area in the Control group was +, while it was ++ in the

Perioderm group and +++ in the Axolotl group. These findings suggest that the Axolotl group, as compared to the Perioderm group and Control group at 21, 30 days, showed a greater ability to regenerate/heal new tissue in the wounded area (+++) (Figures 15 on 30 days, black arrows)

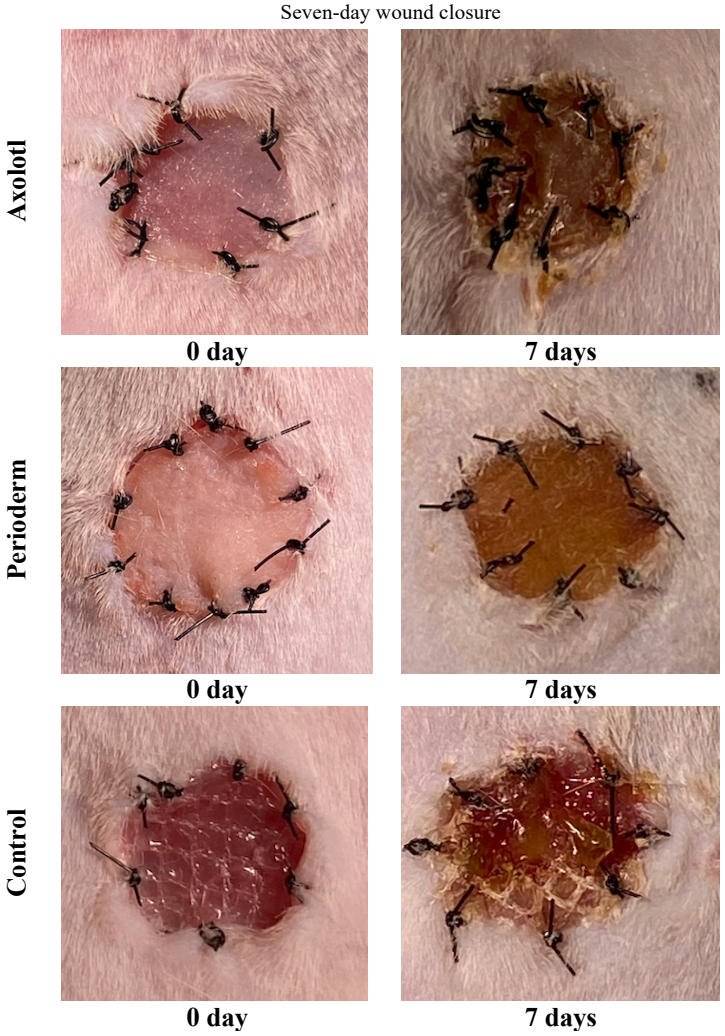

Figure 14 In a 7-day experiment, an 8-millimeter circle wound was made on the dorsal of the mice using a punch biopsy, and images were taken on days 0 and 7. At 7 days, there was no difference in wound closure between Axolotl, Perioderm, and Control groups.

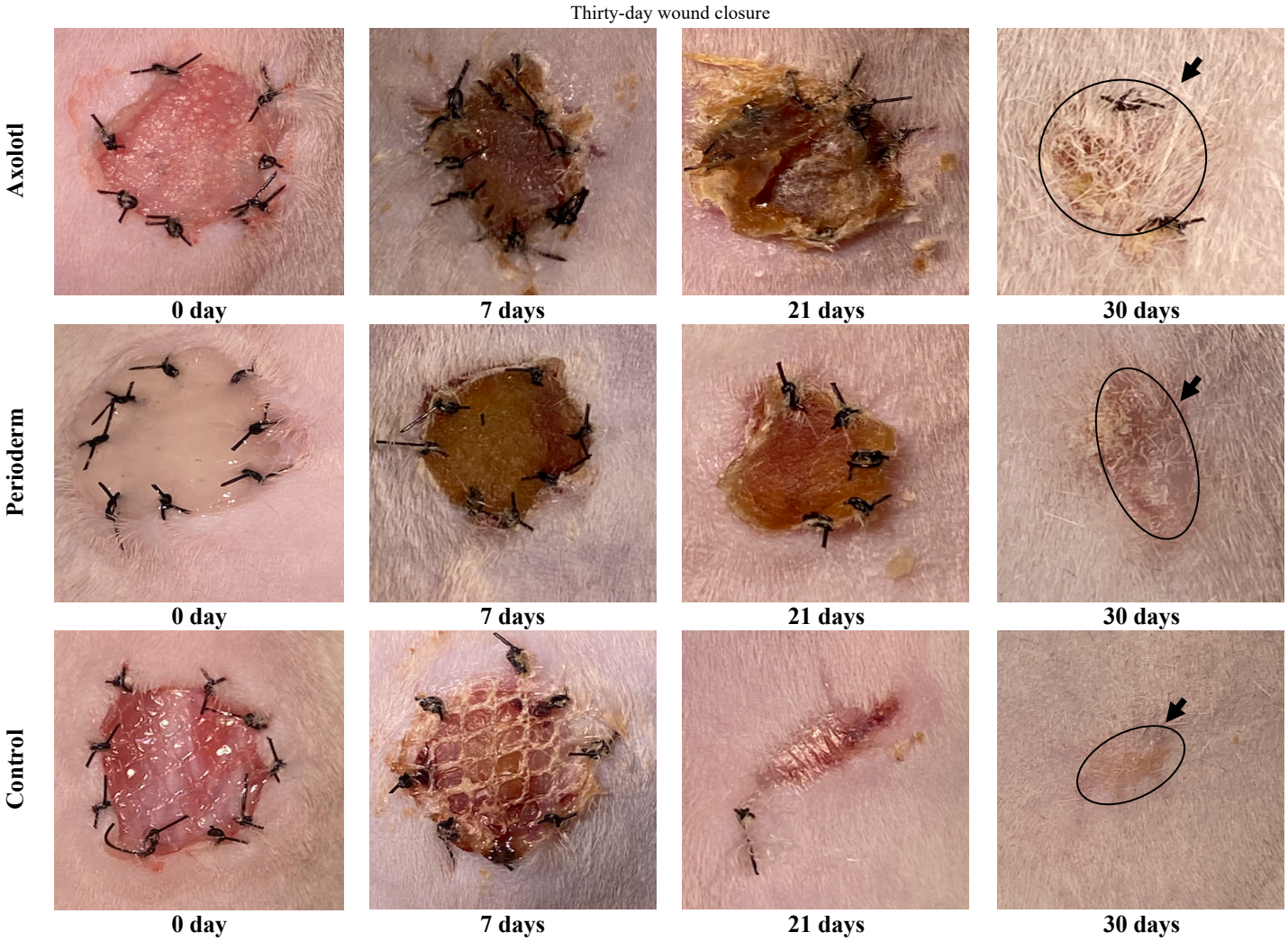

Figure 15 In a 30-day experiment, a punch biopsy was used to make an 8 mm circle wound on the dorsa of the mice, and photographs were taken at 0,7,21, and 30 days after the wound was made. In the axolotl, Perioderm, and control groups, there was difference in closure rate at 7 days. But there were differences in wound closure (tissue closure) and new tissue over the wounded area between the Axolotl, Perioderm, and control groups on days 21, 30. The percentage of tissue closure was ++ large in the Control group, while the percentage of tissue closure was + in the Perioderm and Axolotl groups on days 21, however, the percentage of tissue closure was +++ in all the groups on 30. On days 21 and 30, the percentage of new tissue over the wound area in the Control group was +, while the percentage of new tissue over the wounded area was ++ in the Perioderm group and +++ in the Axolotl group.

	Time points	0 day	7 days	21days	30 days
Axolotl group	WC	–	–	+	+++
	NTOWA	–	–	+++	+++
Perioderm group	WC	–	–	+	+++
	NTOWA	–	–	++	++
Control group	WC	–	–	++	+++
	NTOWA	–	–	+	+

Scoring of WC: Wound Closure; NTOWA: New Tissue Over Wounded Area

The macroscopic scale, semi quantitative analysis results of Wound closure (Table 2)

3.2.2 Trans-illumination Test

A trans-illumination test was used to observe the development of microvascular networks within and along the wound margins and grafts in both seven-day and thirty-day experiments. In general, there was a noticeable difference between the vascular networks of the Axolotl, Perioderm, and Control groups in the seven-day experiment (Figure 16) (Table 3).

The microvascular network was +++ at the center and edges of the Axolotl's wounds (Figures 16A, B black/white arrows), whereas it was + only at the edges in the Perioderm and Control groups (Figures 16C, D) 16D, E, G, H black /white arrows). Further, in 7-day experiment, the color of the tissue covering the back wounds varied markedly among the Axolotl, Perioderm, and Control groups. On the backs of the Axolotl wounds, the tissues were more reddish in color and more vascularized (++) (Figure 15C black arrow), whereas tissue in the Perioderm and Control groups were more yellowish and showed only a minimal amount of vascularity (+) (Figures 15F, I black arrows).

As determined by the transillumination test in thirty-day experiments, the Axolotl, Perioderm, and Control groups demonstrate different microvascular networks. Microvascular networks in the Axolotl group were +++, whereas those in the Perioderm and Control groups were – (Figures 17A, B, C) (Table 3). As a result of these findings, the Axolotl group was more able to create vascular networks (+++) in the wounded area than the Perioderm group and Control group at 7 and 30 days (Figure 17, 16) (Table 3).

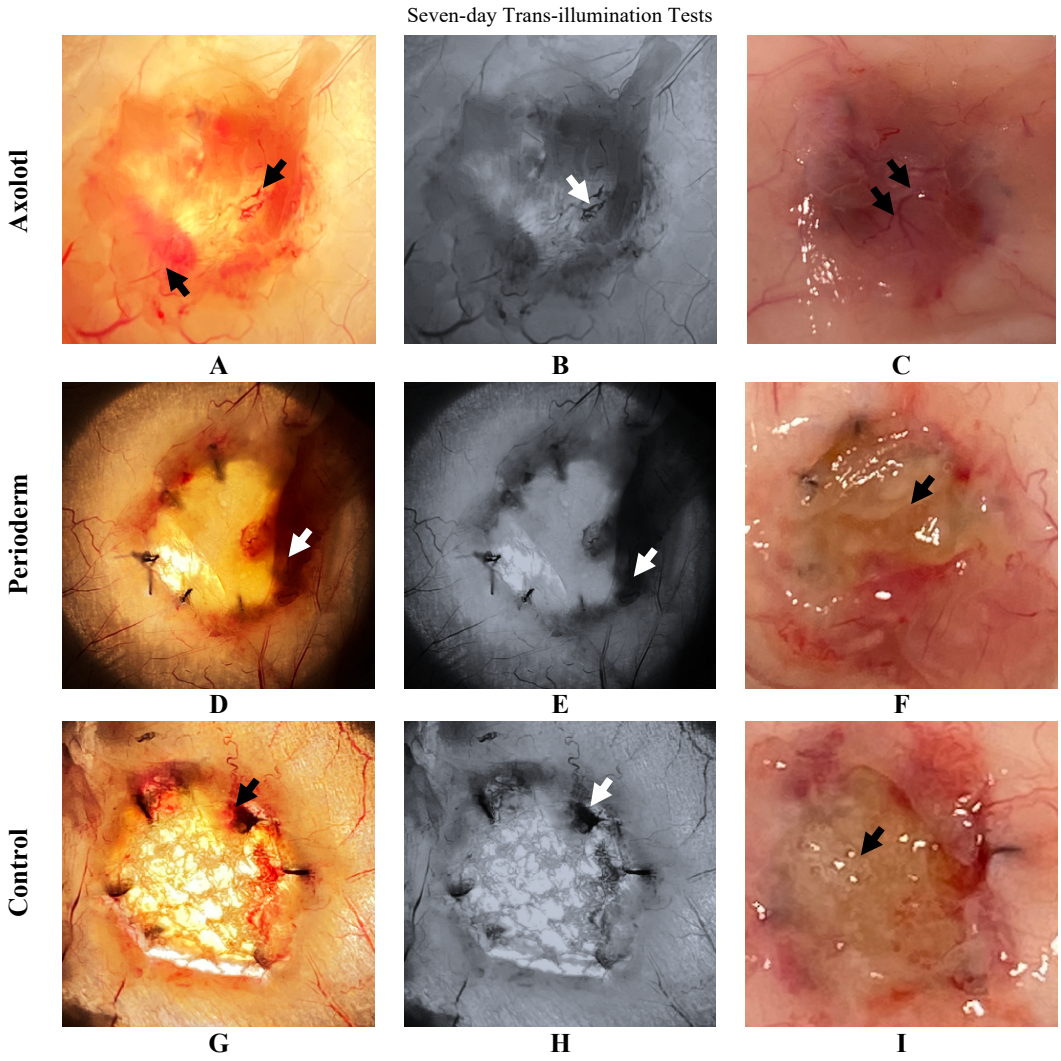

Figure 16 In a 7-day experiment, Axolotl group (A, B) showed +++ vascular network, whereas Perioderm group (D, E) and Control group (G, H) did present + vascular network. The tissue back wounds were more reddish in color and showed more vascularity in the Axolotl group (C) and were yellowish in color and showed only minor vascularity in the Perioderm (F) and Control groups (I).

Thirty-day Transillumination Test

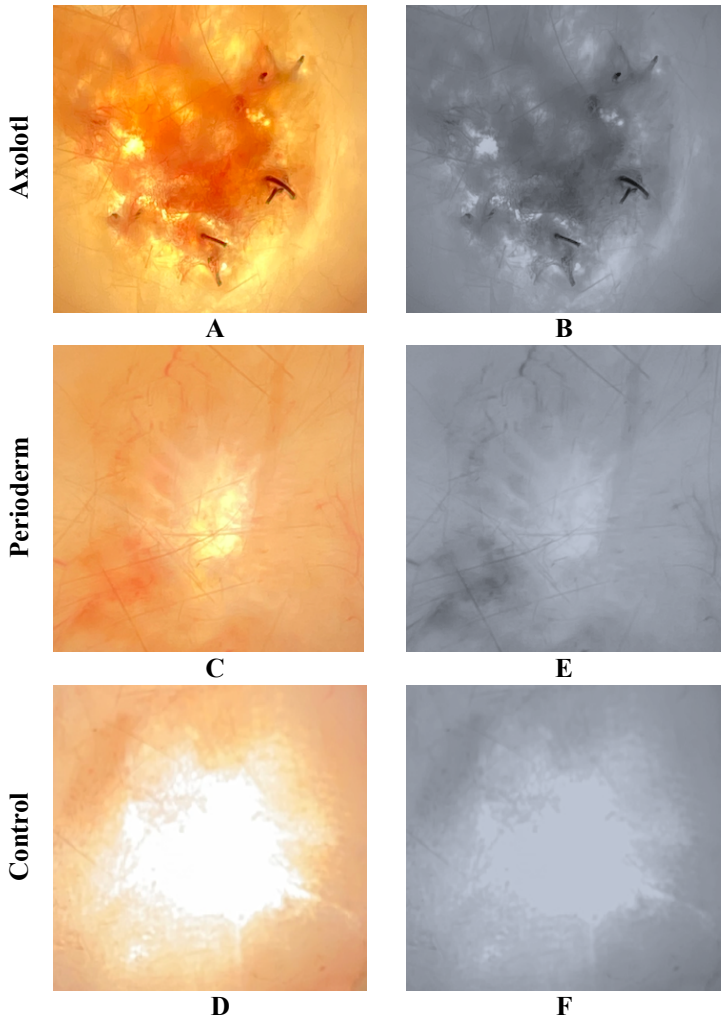

Figure 17 In a 30-day experiment, the Axolotl group (A, B) showed +++ vascular network, whereas the Perioderm group (D, E) and Control group (G, H) did show – vascular network.

	Time points	0 day	7 days	30 days
Axolotl group	VN	–	+++	+++
Perioderm group	VN	–	+	–
Control group	VN	–	+	–

Scoring of VN: vascular networks

The macroscopic scale, semi quantitative analysis results of Transillumination test (Table 3)

3.2.3 Histological analysis

In the seven-day and thirty-day experiments, Sirius and hematoxylin & Eosin were used to examine the histology of the grafts to determine whether collagen and cells were distributed differently in wound areas between the Axolotl, Perioderm, and control groups.

3.2.3.1 Sirius red staining

In scarring regions, the collagen fibers are usually larger, evenly distributed and organized into cross-hatched patterns. Both the seven-day and thirty-day experiments revealed different collagen contents among the Axolotl, Perioderm, and Control groups (Figures 18A, B, C, 20A, B, C, 22A, B, C, 24A, B, C). On 7 and 30 days, the collagen content in the Axolotl group was +++, whereas in the Perioderm group, it was + on 7 days and ++ on 30 days (Figures 19A, C, 21A, C, 23A, C, 25A, C) (Table 4). In contrast, the collagen content of the Control group was ++ on 7 days and + on 30 days (Figures 19D, 21D, 23D, 25D) (Table 4). In addition, new collagen pattern was distributed and arranged into a porous network (spongy-like) on 7 days and 30 days in the Axolotl group (Figures 19A, 21A, 23A, 25A black /white arrows), while new collagen was arranged in linear and wave patterns without porous matrix on days 7 and 30 in the Perioderm group (Figures 19C, 21C, 23C, 25C black /white arrows). The collagen pattern developed in the Control group was arranged linearly and in waves, with less porous on day 7, but no porous on day 30 (Figures 19D, 21D, 23D, 25D black /white arrows).

In the Axolotl group, the porosity of collagen pattern was +++ on 7 days and 30 days, whereas the porosity of collagen pattern in Perioderm was – on 7 and 30 days (table 4). However, the porosity of collagen pattern in the control group was + on 7 days and - on 30 days (table 4). In conclusion, the Axolotl group showed porous collagen patterns and a higher collagen content in the wound

area as compared to the Perioderm and control groups. Accordingly, the porous collagen pattern formed in the Axolotl group could facilitate cell proliferation and differentiation more efficiently than collagen pattern observed in the Periderm and Control groups. (99-101).

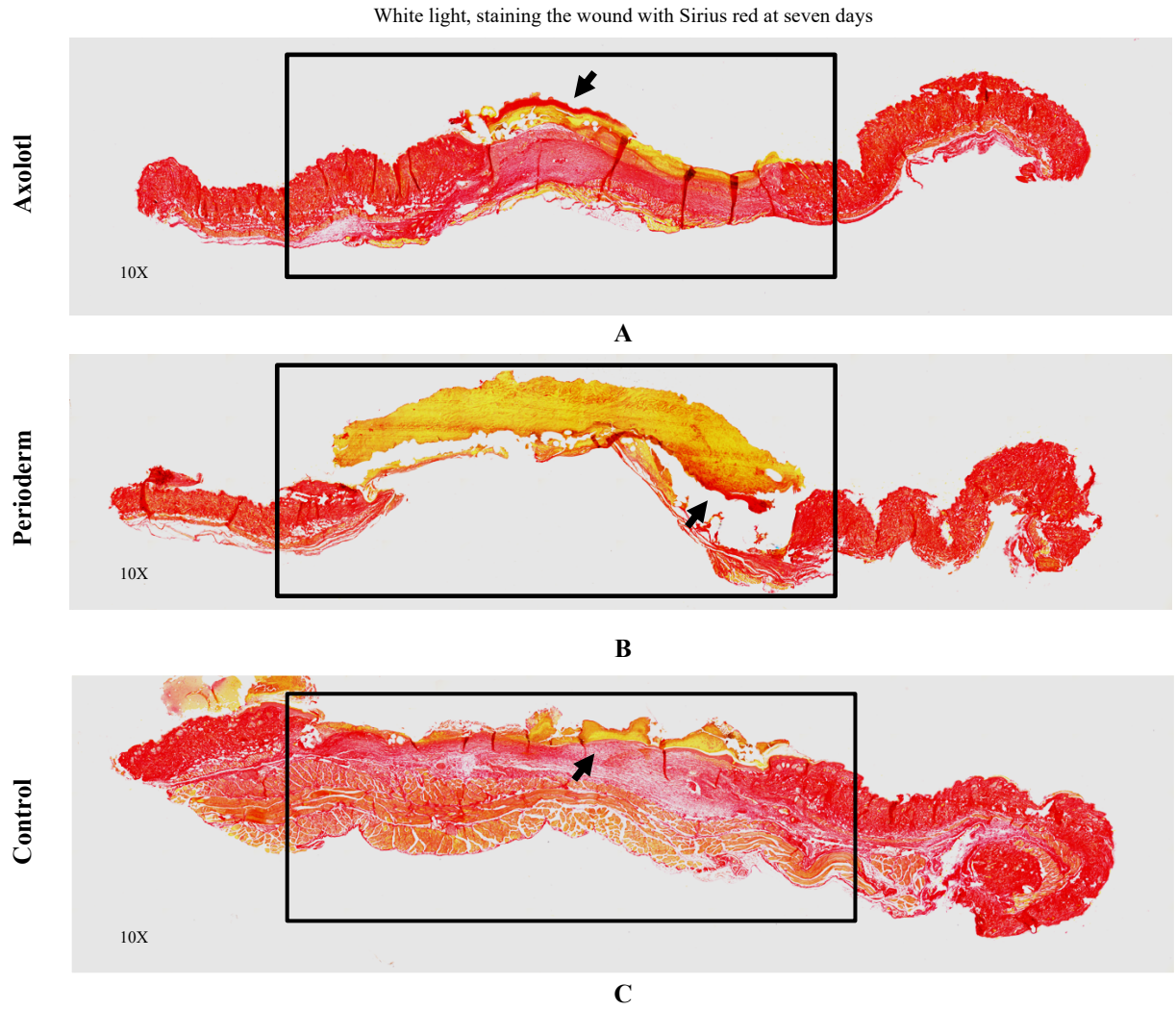

Figure 18 Representative full wound sections in White light, a magnification 10X.The Sirius red stain has been used to examine collagen content and its orientation in healing wounds for each of the Axolotl, Perioderm, and Control groups. The collagen content of the axolotl group was +++ and the matrix formed under the Decellularized Axolotl Skin ECM was oriented in a porous pattern (A). In the PrioDerm group, the amount of collagen was +, but no matrix (B). In the Control group, collagen content was (++), matrix orientation was linear, and porosity was (–) (C).

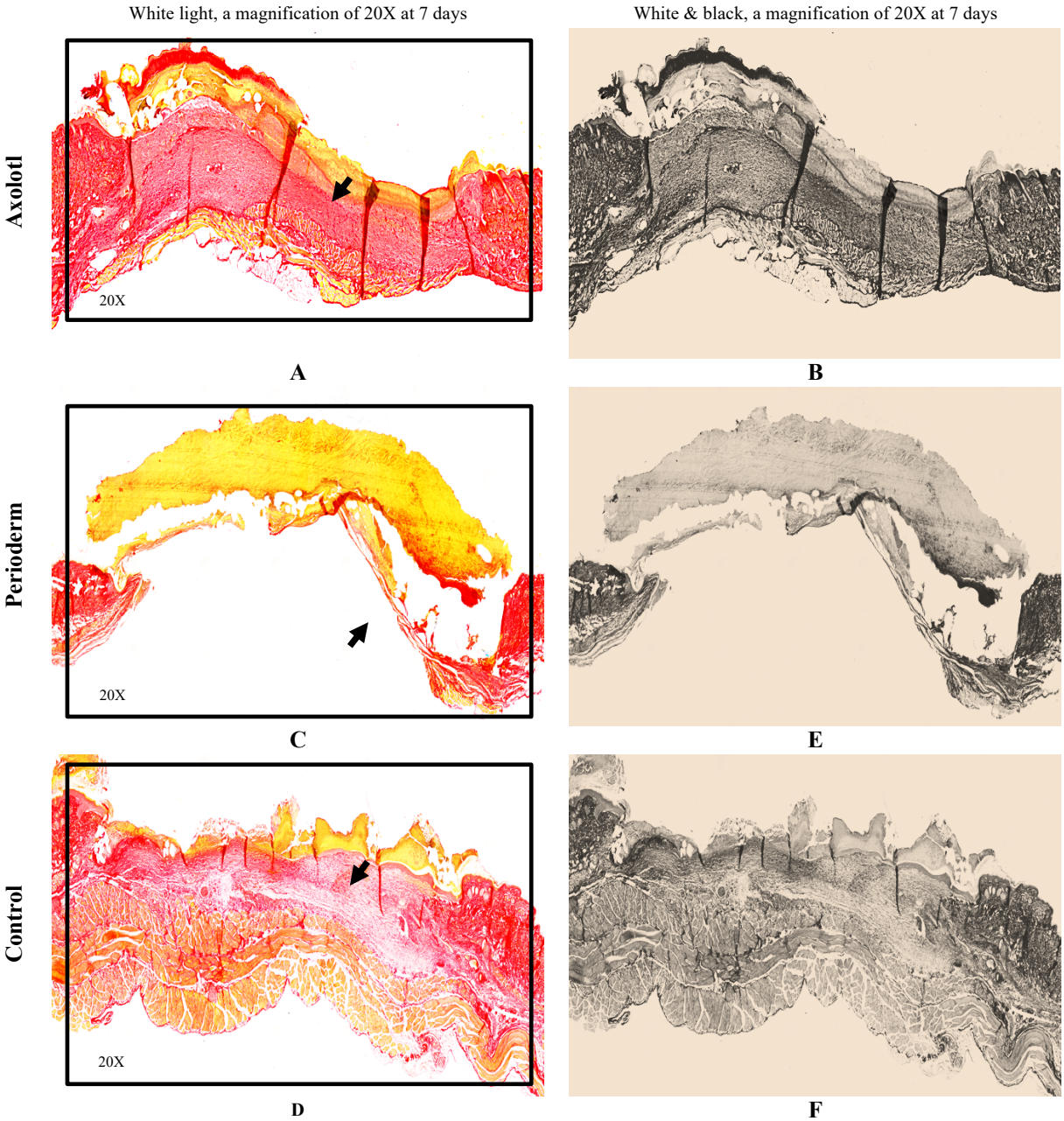

Figure 19 This figure represents high-powered images of the epidermal-dermal border in White light, a magnification 20X. The Sirius red stain was used to measure collagen content and orientation in healing wounds for the Axolotl, PerioDerm, and Control groups. Collagen content was (+++) in the axolotl group, and the porosity of matrix was (+++) (A, B). PrioDerm group, the amount of collagen was (+), but no matrix (C, E). The collagen content in the Control group was (++), and the porosity of matrix was (+) (D, F).

In polarized light, staining the wound with Sirius red at seven days

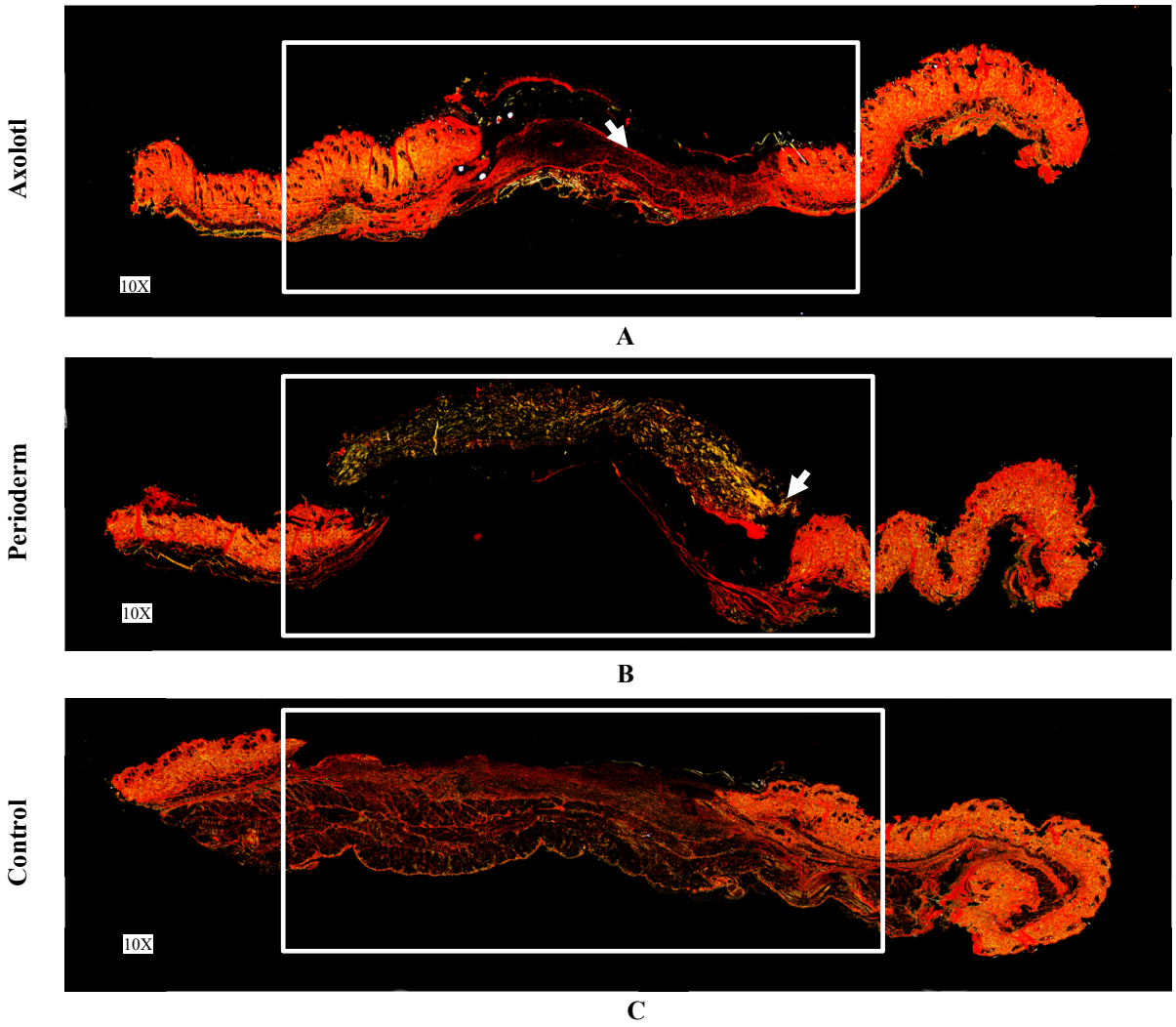

Figure 20 Representative full wound sections in polarization field, a magnification 10X. The Sirius red stain has been used to examine collagen content and its orientation in healing wounds for the Axolotl, PerioDerm, and Control groups. The collagen content of the axolotl group was (+++), and the matrix was oriented in a porous pattern (A). In the PerioDerm group, the amount of collagen was (+), but no matrix (B). In the Control group, collagen content was (++), matrix orientation was linear, and porosity of matrix was (+) (C).

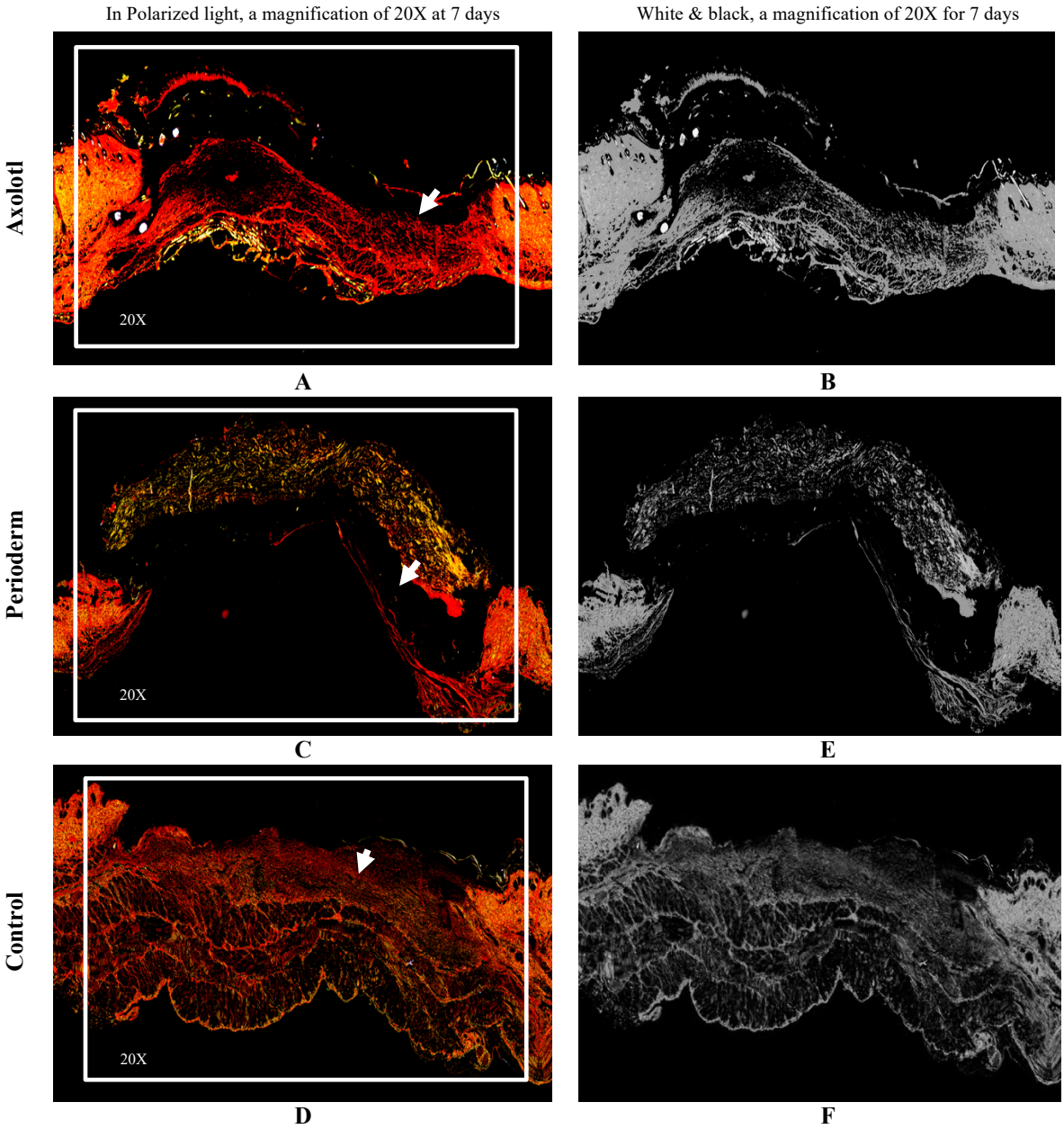

Figure 21 This figure represents high-powered images of the epidermal-dermal border in Polarization light, a magnification 20X. The Picrosirius red stain was used to measure collagen content and orientation in healing wounds for the Axolotl, PerioDerm, and Control groups. Collagen content was (+++) in the axolotl group, and the porosity of matrix was (+++) (A, B). PrioDerm group, the amount of collagen was (+), but no matrix (C, E). The collagen content in the Control group was (++), and the porosity of matrix was (+) (D, F).

White light, staining the wound with Sirius red at thirty days

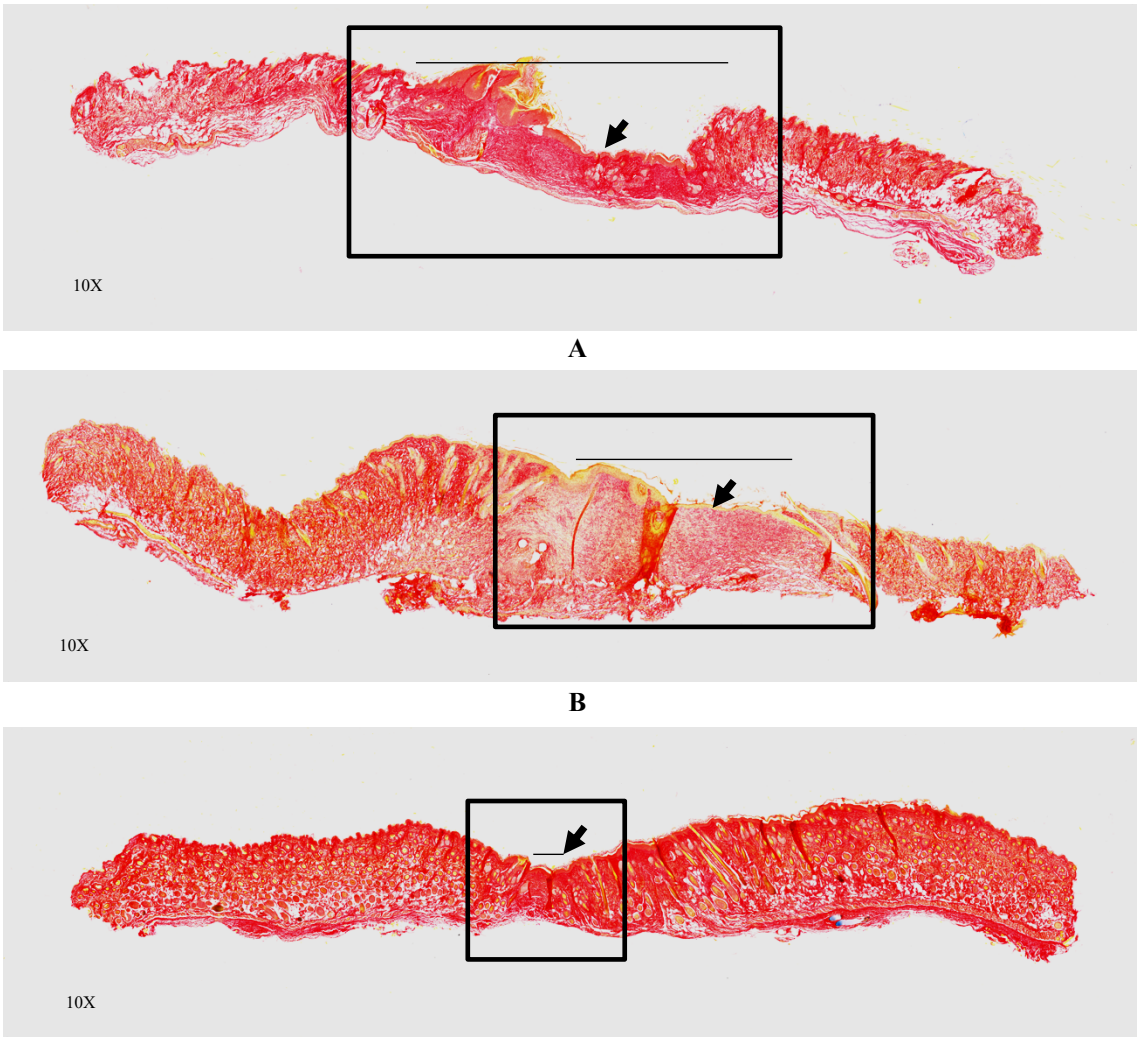

Figure 22 Representative full wound sections in White light, a magnification 10X. The Sirius red stain has been used to examine collagen content and its orientation in healing wounds for each of the Axolotl, Perioderm, and Control groups. In axolotl group, the collagen content was +++ amount and the new matrix collagen formed was porous. Also, new tissue over the wounded area in axolotl group was (+++), in comparison to Perioderm group, it was (++) and Control group, it was (+) (A, B, C). The collagen content in Perioderm group was (++), in which distributed & arranged into linear and wave patterns, with no porous matrix (B). The collagen content in the control group was (+), in which arranged in a cross-hatched pattern (this could represent scar tissue), matrix was not porous (C).

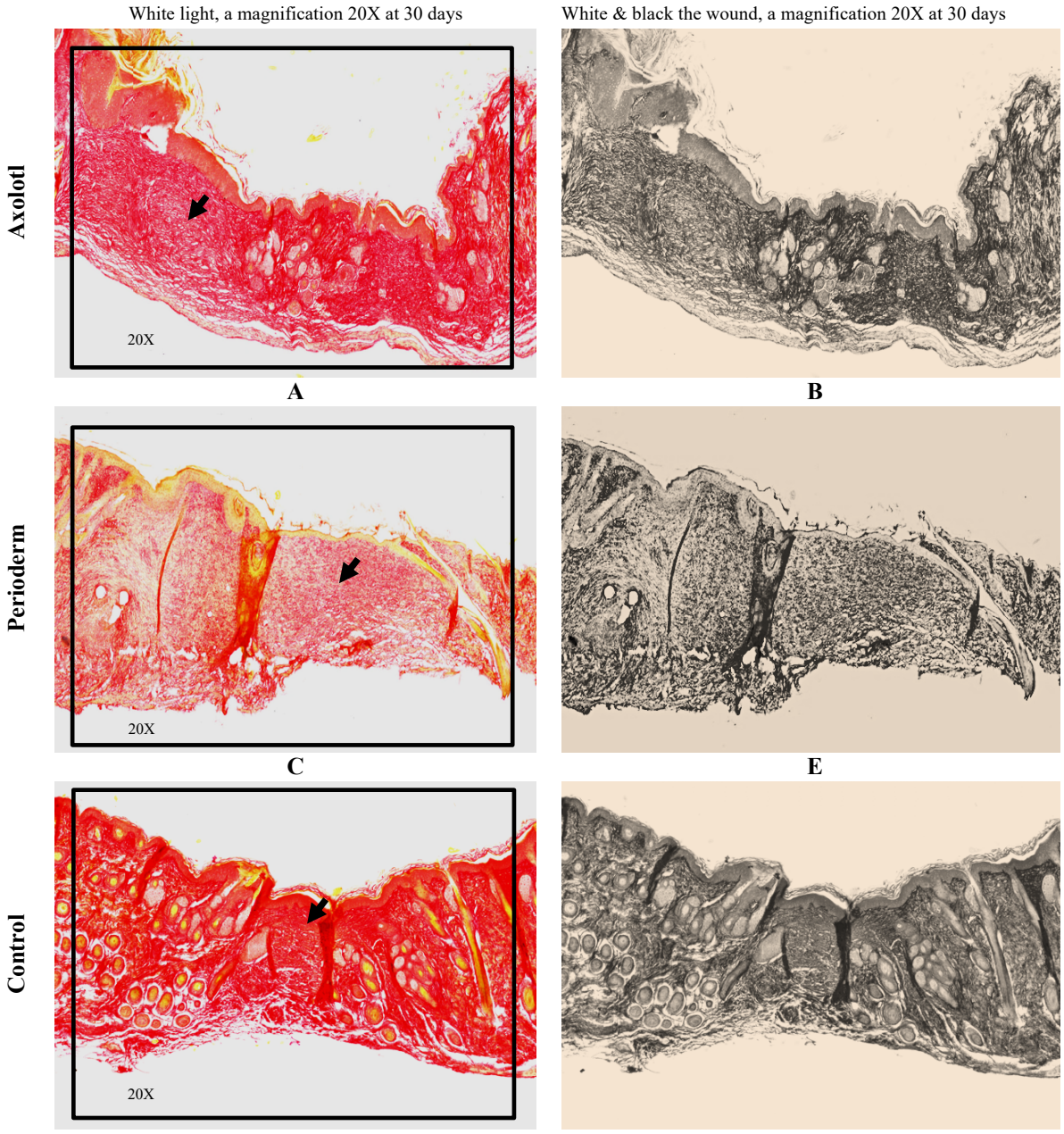

Figure 23 This figure represents high-powered images of the epidermal-dermal border in White light, a magnification 20X. The Sirius red stain was used to measure collagen content and orientation in healing wounds for the Axolotl, PerioDerm, and Control groups. In the axolotl group, the collagen content was +++ amount, and the matrix was oriented in a porous manner (A, B). In the PrioDerm group, Collagen content was (+++) in the axolotl group, and the porosity of matrix was (+++) (A, B). PrioDerm group, the amount of collagen was (++), and the porosity of matrix was (–) (C, E). The collagen content in the Control group was (+), and the porosity of matrix was (–) (D, F).

In polarization field, staining the wound with Sirius red at thirty days

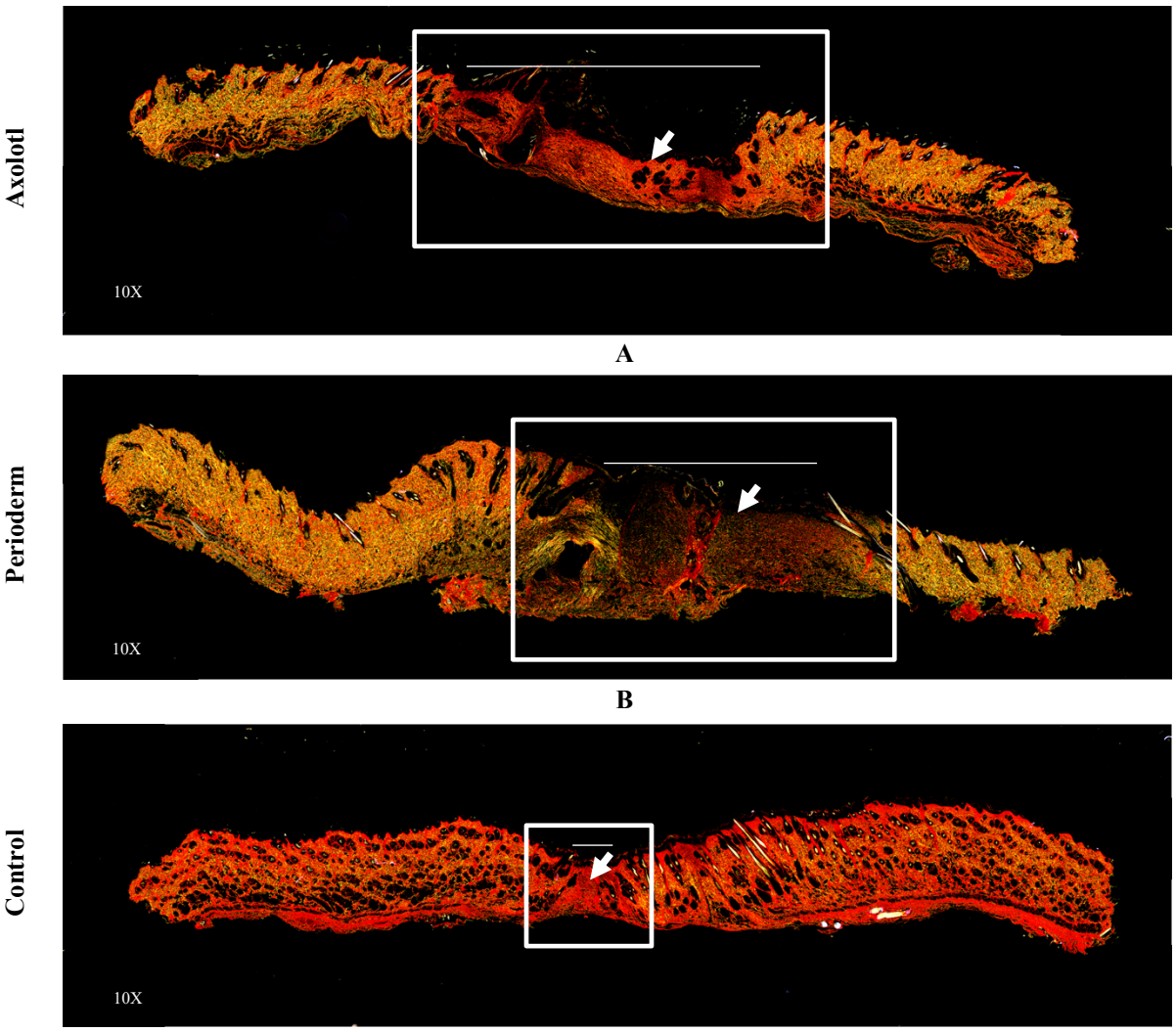

Figure 24 Representative full wound sections in polarization field, a magnification 10X. The Sirius red stain has been used to examine collagen content and its orientation in healing wounds for each of the Axolotl, Perioderm, and Control groups. In axolotl group, the collagen content was +++ amount and the new matrix collagen formed was porous. Also, new tissue over the wounded area in axolotl group was (+++), in comparison to Perioderm group, it was (++) and Control group, it was (+) (A, B, C). The collagen content in Perioderm group was (++), in which distributed & arranged into linear and wave patterns, with no porous matrix (B). The collagen content in the control group was (+), in which arranged in a cross-hatched pattern (this could represent scar tissue), matrix was not porous (C).

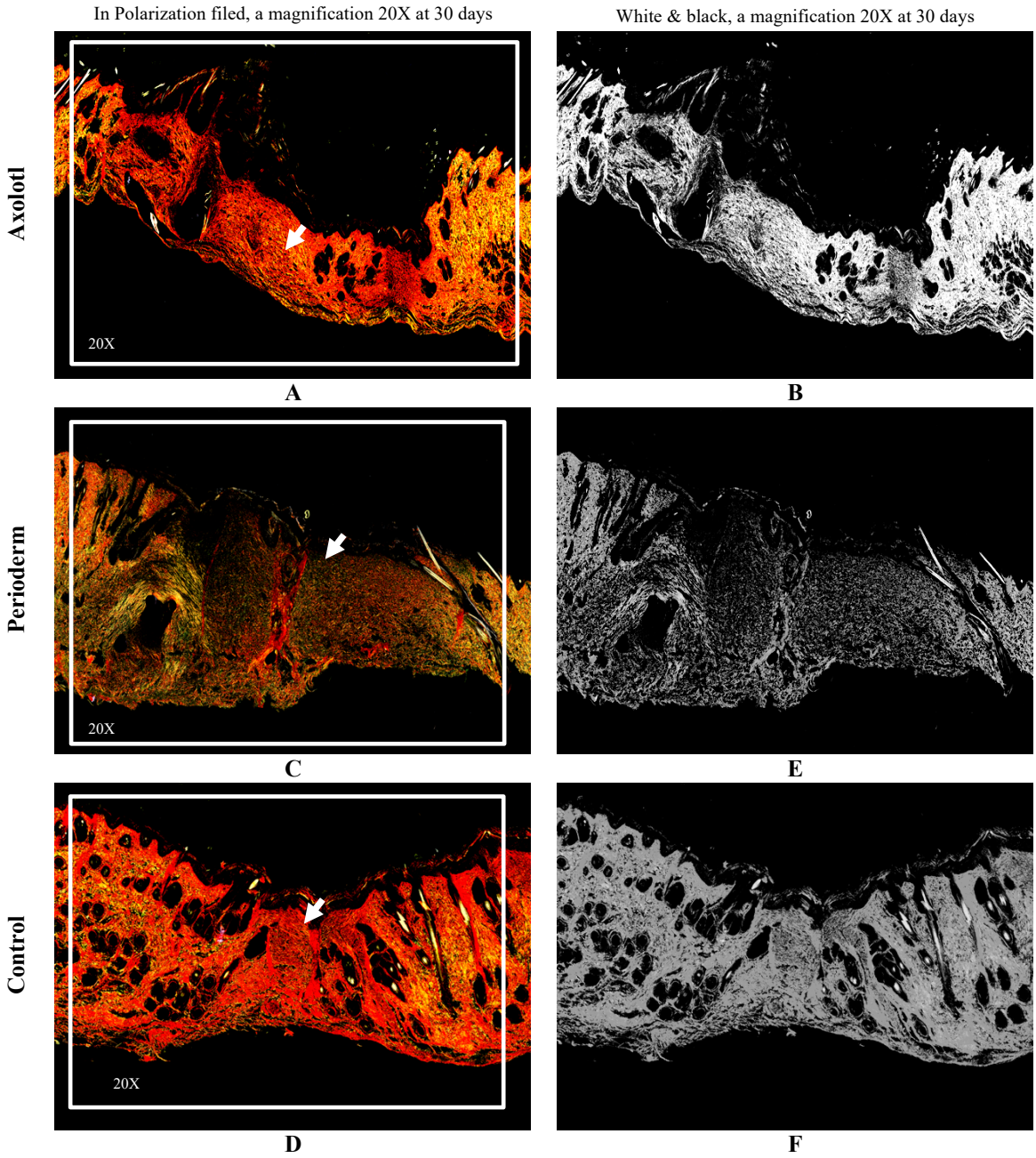

Figure 25 This figure represents high-powered images of the epidermal-dermal border in Polarization field, a magnification 20X. The Sirius red stain was used to measure collagen content and orientation in healing wounds for the Axolotl, Perioderm, and Control groups. In the axolotl group, the collagen content was +++ amount, and the matrix was oriented in a porous manner (A, B). In the Perioderm group, Collagen content was (+++) in the axolotl group, and the porosity of matrix was (+++) (A, B). Perioderm group, the amount of collagen was (++), and the porosity of matrix was (–) (C, E). The collagen content in the Control group was (+), and the porosity of matrix was (–) (D, F).

	Time points	0 day	7 days	30 days
Axolotl group	CC	–	+++	+++
	CP(P)	–	+++	+++
Perioderm group	CC	–	+	++
	CP(P)	–	–	–
Control group	CC	–	++	+
	CP(P)	–	+	–

Scoring of CC: Collagen Content; CP(P): Collagen Pattern (Porosity)

The microscopic scale, semi quantitative analysis results of Sirius red (Table 4)

3.2.3.2 Hemoxylin & Eosin staining

Hematoxylin and eosin staining was used in both the seven-day and thirty-day experiments to demonstrate the migration of cells in the wound area (Figures 26, 27, 28,29). Both the seven-day and thirty-day experiments revealed different epithelial cells among the Axolotl, Perioderm, and Control groups. On 7 and 30 days, the epithelial cells (epithelium layer) in the Axolotl group were +++, whereas in the Perioderm group, it was + on 7 days and ++ on 30 days (Figures 26A, B, 27A, C, 28A, B, C, 29A, C, D). (Table 5). In contrast, the epithelial cells (epithelium layer) in the Control group were ++ on 7 days and + on 30 days (Figures 26C, 27D, 28C, 29D) (Table 5)

In the center of the wound, the epidermal layer, basal lamina, and connective tissue (dermal layer) were +++ after 7 days and 30 days (figure 27B, 29A (III)(V) black arrows, 29A black arrow). Contrary to this, the epidermal layer, the basal lamina, and the connective tissues (dermal layer) in the center of the wound were all ++ after 7 days and ++ after 30 days in the Periderm group (figures 27C, E, 29C, E) (Table 5). The epidermis, basal lamina, and connective tissues (dermal layer) in the control group were all ++ after 7 days and at 30 days (figures 27D, F, 29D, F) (table 5).

In the Axolotl group, a reddish spot in the connective tissue was + after 7 days, suggesting dense vascularization (figure 27B, (I) (II) black arrows). The Axolotl group did not have any reddish spots after 30 days and neither did the Perioderm group or the control group on 7 and 30 days. On day seven, *the panniculus carnosus muscle* was ++ under the connective tissue at the center of the Axolotl wound (figures 26A (I) black arrow, 27B (IV) black arrow). Whereas *the panniculus carnosus muscle* was – in the wound area in the Perioderm group on 7 and 30 days (Table5). In contrast, *the panniculus carnosus muscle* in the Control group was + under the connective tissue

after 7 days (figure 27D (I) black arrow). After 30 days, none of the Axolotl, Perioderm, or Control groups showed any signs of *the panniculus carnosus* in the wound area (Table5).

Interestingly, on 7 and 30 days, cell density (epithelium and dermal layers) in the Axolotl group was +++, whereas in the Perioderm group, it was + at 7 days and ++ at 30 days (Figures 26A, B, 27A, C, 28A, B, C, 29A, C, D). (Table 5). And cell density (epithelium and dermal layers) in the Control group was ++ at 7 and 30 days (Figures 26C, 27D, 28C, 29D) (Table 5).

Also, Axolotl groups showed some dermal appendages at 30 days, including hair follicles, sweat glands, apocrine glands, and sebaceous glands (Figure 29B, (I)(II)(III) black arrows). Hair follicles and sebaceous glands were + on day 30 in the center of the axolotl wound (Figure 29B) (Table 5). Axolotls, however, lacked dermal appendages (hair follicles and sebaceous glands) on day 7 (Figure 27B). Moreover, neither the Perioderm nor the Control groups showed signs of dermal appendages (hair follicles or sebaceous glands) within the wound area after 7 and 30 days (Figures 27C, E, D, F 29C, E, D, F) (Table 5).

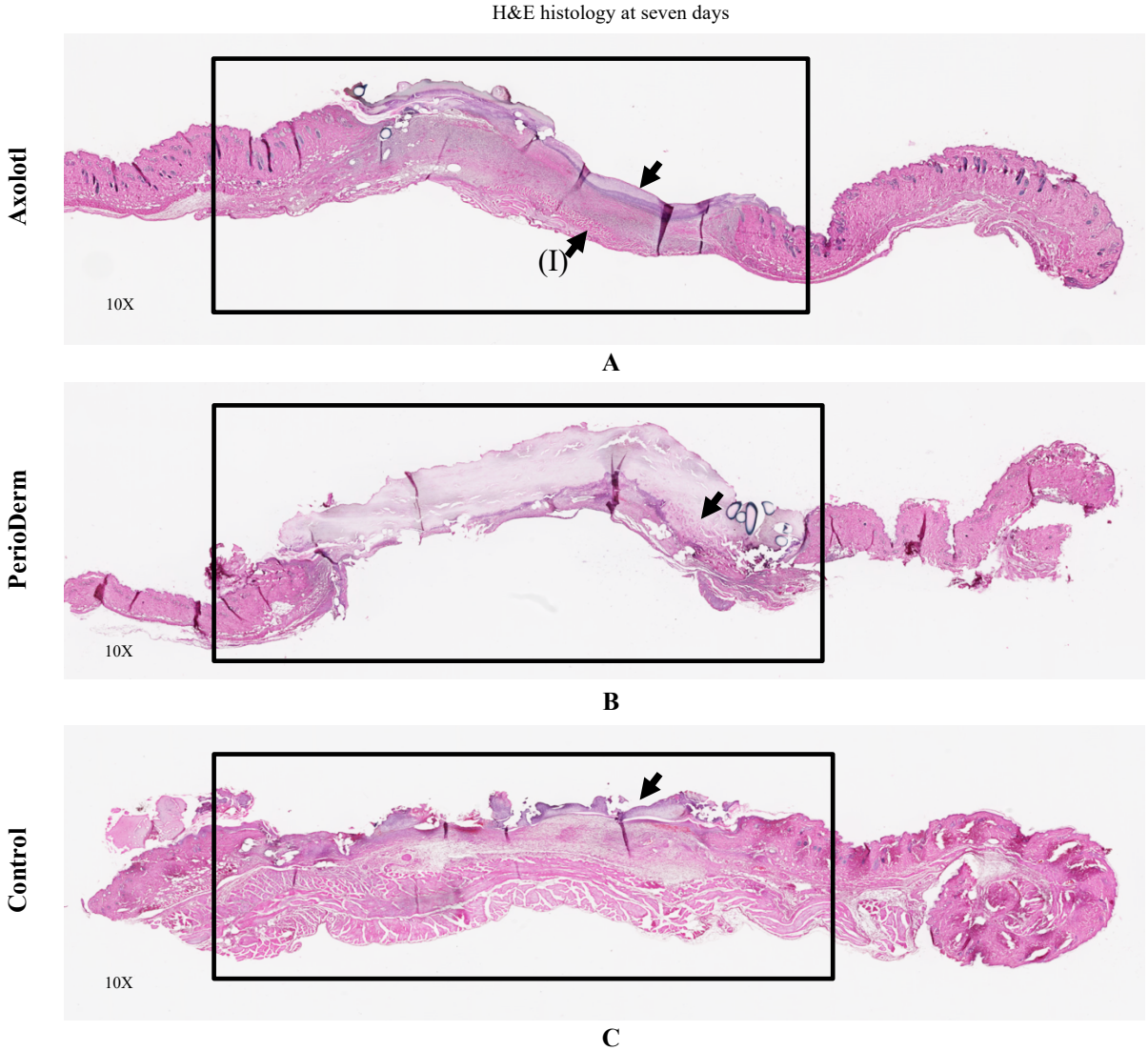

Figure 26 Representative full wound sections, a magnification 10X. The slides were stained with hematoxylin and eosin to demonstrate the cellular presence in the granulation tissues in the wound areas of each of the three groups: Axolotl, Perioderm, and Control. The wound was completely re-epithelialized in the Axolotl group (A), Under the connective tissue at the center of the wound, parts of *the panniculus carnosus* have grown (I) black arrow. In the Periderm group, the wound surface was poorly re-epithelialized (B). In the Control group, the wound surface was incompletely re-epithelialized and covered with ++ amount epithelial cells(C)

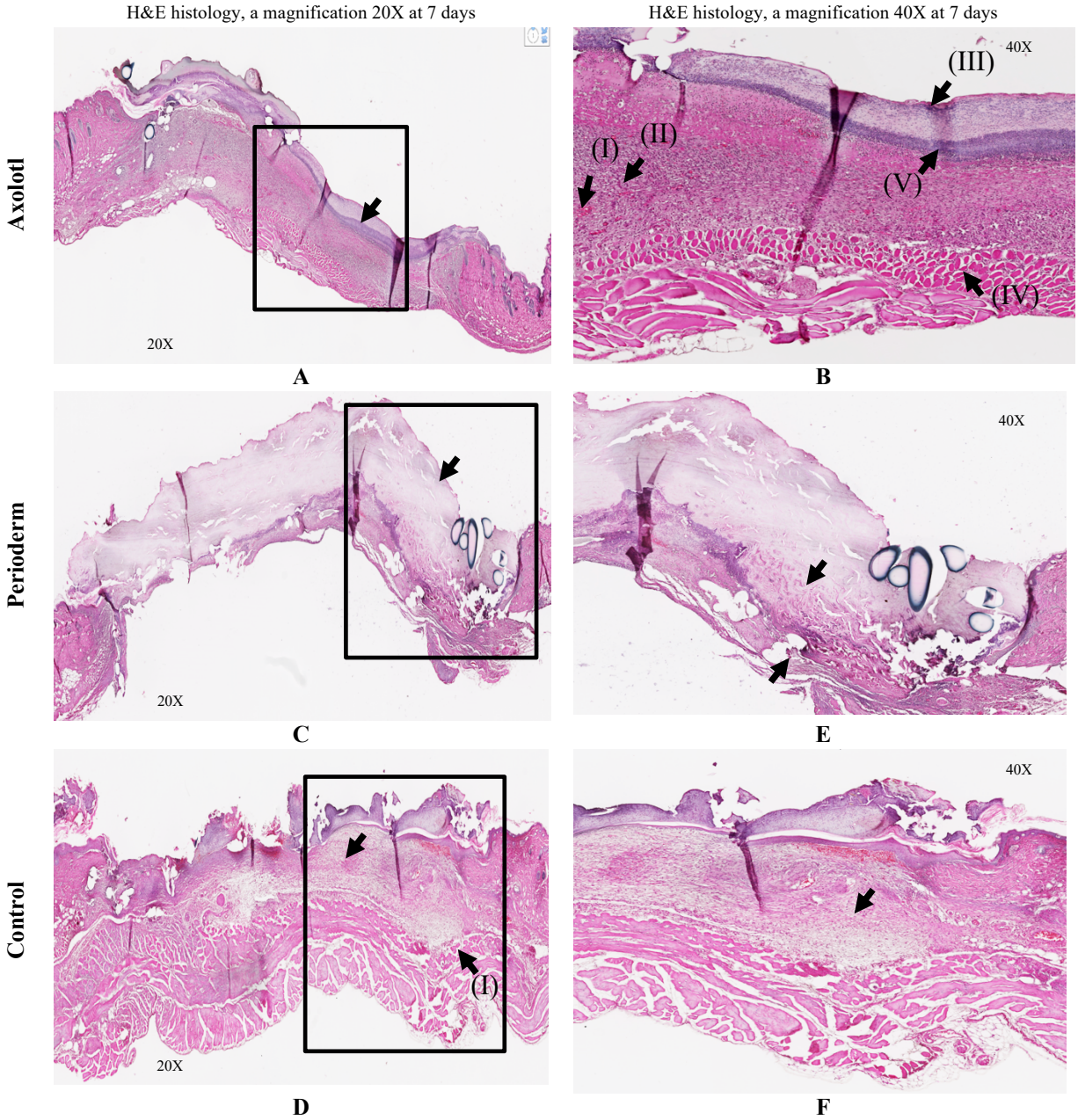

Figure 27 This figure represents high-powered images of the epidermal-dermal border, a magnification 20X, 40X. Hematoxylin and eosin staining was used to show granulation tissue cells in wound areas of the three groups: Axolotl, Perioderm, and Control. Cell density was +++ in the center of axolotl's wounds (A), A reddish spot was seen in the central area of the wound, possibly indicating dense vascularization (B, (I)(II)black arrows), A +++ amount of epidermal thickness, basal lamina, and connective tissue were observed in the wound center (B, (V)(III)black arrows), Part of *the panniculus carnosus* muscle have grown under the connective tissue in the center of the wound (B, (IV)black arrow). Cell density was + in the center of Perioderm's wounds (C, E). In Control group, cell density was ++ in the center of wounds (D), *A panniculus carnosus* muscle may have been observed slightly under the connective tissue (D (I)black arrow).

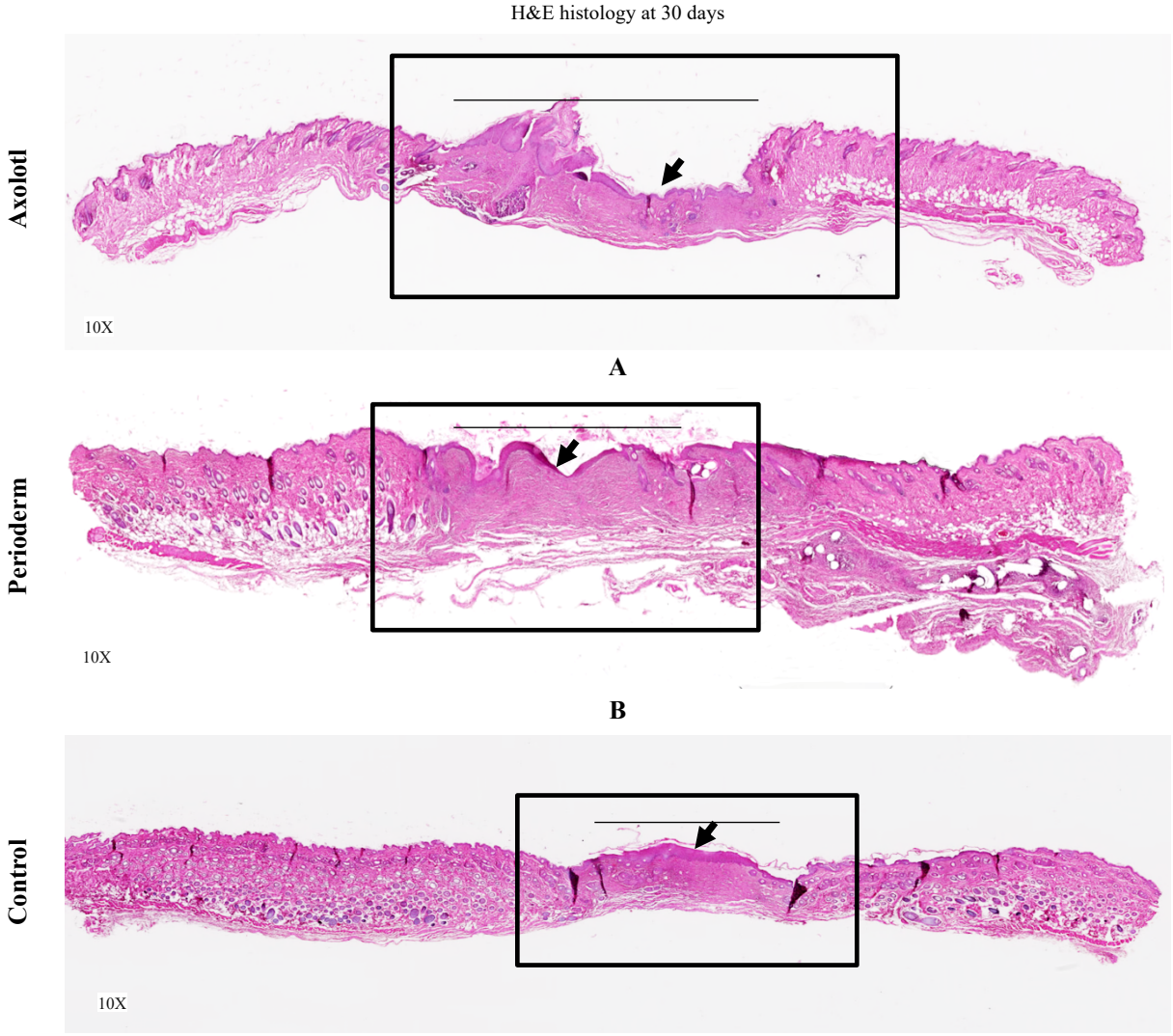

Figure 28 Representative full wound sections, a magnification 10X. For the purposes of demonstrating the cellular positions in the granulation tissues of the wounds, of each of the three groups: Axolotl, Perioderm, and Control, the slides were stained with hematoxylin and eosin. Axolotl wounds were epithelized, and *the panniculus carnosus muscle* was not visible beneath the dermis (A). In the Perioderm group, the wound surfaces were epithelized, and *the panniculus carnosus muscle* did not appear under the dermis (B). In the Control group, the wound surfaces were epithelized, and *the panniculus carnosus muscle* was not evident under the dermis (C).

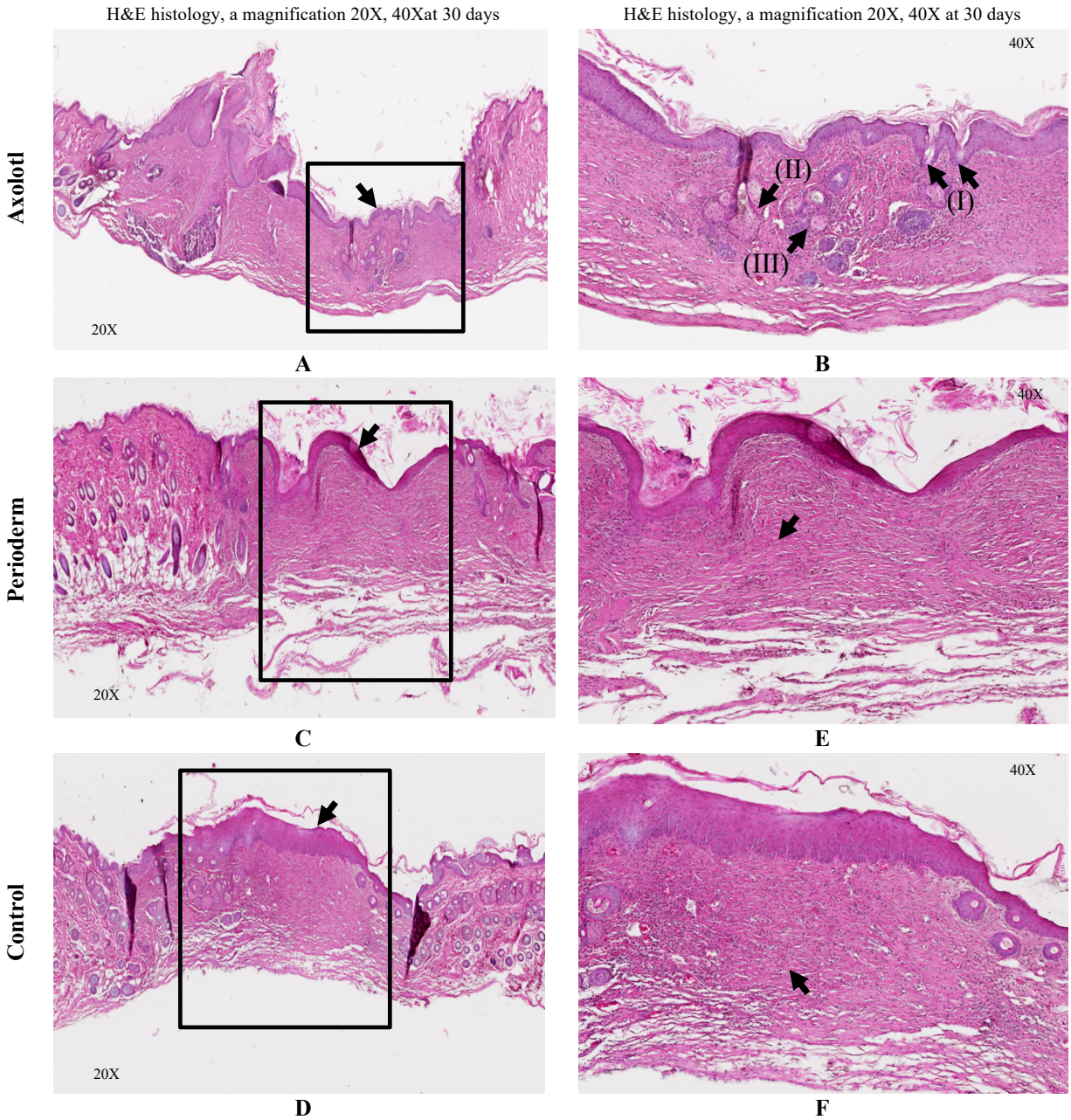

Figure 29 This figure represents high-powered images of the epidermal-dermal border, a magnification 20X, 40X. Hematoxylin and eosin staining was used to show granulation tissue cells in wound areas of the three groups: Axolotl, Perioderm, and Control. The epidermal thickness, basal lamina, and connective tissues at the wound site in the axolotl group were +++ (A), there were some dermal appendages in the center of axolotl's wounds, probably hair follicles, sweat glands (eccrine), apocrine glands, and sebaceous glands (B, (I)(II)(III) black arrows). In the Perioderm group, epidermal thickness, basal lamina, and connective tissues were ++ (B). In the Control group, the epidermis thickness, the basal layer, and the connective tissue were ++(C).

	Time points	0 day	7 days	30 days
Axolotl group	EC	–	+++	+++
	EL, BL, CT(DL)	–	+++	+++
	RS	–	+	–
	PCM	–	++	–
	CD	–	+++	+++
	HF, SG	–	–	+
Perioderm group	EC	–	+	++
	EL, BL, CT(DL)	–	+	++
	RS	–	–	–
	PCM	–	–	–
	CD	–	+	++
	HF, SG	–	–	–
Control group	EC	–	++	+
	EL, BL, CT(DL)	–	++	++
	RS	–	–	–
	PCM	–	+	–
	CD	–	++	++
	HF, SG	–	–	–

Scoring of EC: Epithelial cells; EL, BL, CT(DL): Epidermal layer, Basal lamina, and Connective Tissue (Dermal layer); RS: Reddish spot; PCM: *The Panniculus Carnosus Muscle* (Muscle Layer); CD: Cell Density; HF, SG: Hair follicle, and Sebaceous Gland.

The microscopic scale, semi quantitative analysis results of Hematoxylin & Eosin (Table 5)

CHAPTER IV

DISCUSSION

Axolotls' ECM matrix was decellularized by using the procedure in (Table 1). This method is commonly used to decellularize tissue matrix because it is less damaging to matrix proteins (102). It is essential that the ECM be free of all cells and cellular debris in order to minimize rejection by the immune system of the host animal as much as possible. Studies have shown that insufficient decellularization is the major cause of scaffold rejection (103).

Thus, it was essential to ensure the Axolotl ECM matrix was free from nuclei and cellular debris (102), which can be determined by testing for the presence of genomic DNA with PCR and staining with DAPI. In the PCR test, both decellularized Axolotl Skin ECM and blank water (Negative control) did not show any DNA bands, while intact skin showed an intense band. Consequently, in ECM from decellularized axolotl skin cells were removed, while intact axolotl skin (positive control) displayed the presence of genomic DNA and cells. Staining with DAPI confirm the same finding. Interestingly, we showed that decellularized axolotl skin is well tolerated in mammalian models, as there is no sign of rejection.

The decellularization of skin ECM is inevitably accompanied by some degree of damage to the structural proteins, so Sirius red and indirect immunofluorescence methods were used to evaluate whether any damage had occurred following the decellularization procedure. The integrity of the extracellular matrix plays a critical role for colonization and proliferation of host cells, as well as promoting regenerative responses (for example, the presence of growth factors, glycoproteins, fibronectin, etc.) (102).

As shown on result page 42, collagen fibers were still readily visible in the decellularized axolotl skin ECM after staining with Sirius Red. Thus, the collagenous matrix structure of the decellularized axolotl skin ECM was maintained after decellularization. As shown in the result section on page 46, collagen IV fibers were visualized using primary antibodies against type IV

collagen in decellularized axolotl skin ECM. This indicates that collagen IV fibers were well preserved after decellularization.

Trans-illumination revealed a highly vascular network at the middle and edge of the Axolotl wounds compared to the Perioderm and Control wounds at 7- and 30-days post-grafting. On day seven, the tissues on the backs of the axolotl wounds appeared more reddish and vascularized than those in the Perioderm and control groups. Both Perioderm and Control groups showed a small number of vascular networks only at the wound edges on day seven and not at 30 days. The revascularization of the wound site is highly beneficial since it nourishes and oxygenates the cells and prevents the development of Ischemia-Reperfusion injuries. As an example, diabetic wounds are susceptible to hypoxia (low oxygen levels) as a result of inadequate angiogenesis and the associated vascular dysfunction and neuropathy (104).

Many types of cells secrete VEGF for the purpose of stimulating endothelial cells to produce new blood vessels. Thus, VEGF regulates the migration, proliferation, and differentiation of endothelial cells by interacting with its receptor (105, 106). A lack of angiogenesis due to impaired endothelial function also inhibits fibroblast proliferation and collagen deposition by preventing the hydroxylation of proline and lysine residues, which negatively affects scarring outcomes (107). It is possible that VEGF expression is higher in the axolotl groups and future experiments could focus on this important angiogenic factor to determine whether this is the case. Consequently, adequate angiogenesis promotes re-epithelialization, fibroblast proliferation, and neutrophil activity in the fight against infection. Thus, axolotls could promote wound healing by forming new blood vessels at the wound site.

In both the first and second experiments, wound closure were not different between the Axolotl, Perioderm, and control groups after 7 days. As shown on result page 49, on days 21 and 30, there

was a difference between the Axolotl, Perioderm, and Control groups in terms of wound closure and new tissue over the wounded area. Despite earlier differences in closure rate, the wounds in the Axolotl, Perioderm, and Control groups were completely closed within 30 days, but the new tissue over the wounded area at the wound site varied between the groups. After 30 days, the new tissue over the wounded area in the axolotl group was +++ as compared to Perioderm (++) and Control (+) groups. As a consequence of these findings, the Axolotl group showed greater tissue regeneration (+++ new tissue over the wounded area) than either Perioderm or the Control group after 30 days (Figures 15 on 30 days) (Figures 22A, B, C, 24A, B, C).

As compared to Perioderm and Control groups, the collagen content and the porosity of new collagen matrix in the Axolotl group were +++ in the wound area (Figure 21A, 25A) , as shown on result page 57. The porosity of a scaffold affects nutrients supply, gas exchange, metabolic waste removal, cell adhesion, and intracellular signaling (108-110). Thus, newly formed collagen patterns in the axolotl group were organized to create a porous network, which should enhance cell migration and differentiation during wound healing (101, 102). On the other hand, neither the Perioderm nor the control groups demonstrated a high collagen content or a porous network pattern after thirty days post-grafting.

As shown on result page 67, the wound surface of the Axolotl group was more fully epithelized within seven and thirty days than the wound surface of the Perioderm group and the Control group. In addition, the epidermal layer, basal lamina, and connective tissues (Dermal layer) were +++ in the wound center of Axolotl compared to Perioderm and Control group (Table5). Also, the connective tissue in the center of the wound showed a reddish spot, which was possibly vascularization at 7 days post-surgery. Additionally, the connective tissue in the center of the

wound showed some dermal appendages that were possibly hair follicles, sweat glands, and sebaceous glands (Figure 29B).

On day seven, the wound surface in the Control group was incompletely reepithelialized and covered with some epithelial cells (Figure 26C). However, after 30 days, the central area of the wound in the Control group had been adequately reepithelialized covering the wound area (Figure 29F).

In the control group, epidermal layer, basal lamina, and connective tissues (Dermal Layer) were + at the wound center on day 7 (Figure 26D, F). Nevertheless, on day 30, epidermal layer, basal lamina, and connective tissues (Dermal Layer) were ++ in the wound center (Figure 29D, F). The results of the control group were contrary to expectations. Macroscopic observation of the wounds revealed that the wounds appear to have healed better while transillumination revealed less healing. In contrast, in the periderm group, wound surfaces were poorly epithelized (Figure 26C, E), and epidermal layer, basal lamina, and connective tissues (Dermal Layer) were + on 7 and ++ 30 (Table 5). Based on all of these findings, the grafted axolotl ECM matrix displays better regeneration of epithelium, proliferation, and differentiation compared to the Perioderm and Control groups (Table 5).

Interesting to note, at both day 7 and 30 post-grafting, axolotl wounds were completely re-epithelialized compared to Perioderm wounds and control wounds. Moreover, axolotl group wounds showed some hair follicles and sebaceous glands that were not visible in the Perioderm and control groups 30 days post-grafting (Figures 29B, E, F). Decellularized axolotl skin ECM may contain growth factors (this will need to be investigated further in the future) that facilitate cellular migration into the wound bed which neither Perioderm nor Control groups contained. Moreover, decellularized axolotl skin ECM could also be responsible for the development of

dermal appendages, such as hair follicles and sebaceous glands. Also, the density of cells in the epithelium and connective tissue was higher in the axolotl group than in the Perioderm group and control group at both day 7 and 30 post-grafting.

The results of this study suggest that decellularized extracellular matrix from axolotls could facilitate wound healing in mammals by promoting reepithelialization and angiogenesis. Nonetheless, for a complete understanding of wound healing, further investigations will be needed, such as the analysis of TGF-β signaling pathways, which are crucial for wound healing but can also result in abnormal scarring. Also, various components (cellular receptors and intracellular modulators) need to be assessed by immunofluorescence microscopy to determine the levels of TGF-β receptors (ALK5 and TβRII) as well as to measure the levels of phosphorylated and total Smad2 and Smad3 (which are responsible for proliferation and collagen expression). Also, activation of the MAP kinase signaling (which affects proliferation, migration, and differentiation) should be assessed by assessing phosphorylated and total levels of p38, ERK, and JNK (111-113). The Decellularized axolotl skin ECM will need to be further investigated to determine whether it can enhance reepithelialization, granular tissue formation, vascularization, and even the presence of hair follicles.

CHAPTER V

CONCLUSIONS

The objective of this research, which has never been done in the world before, was to determine whether the ECM scaffolds from axolotls can influence a regenerative response in mammals.

In the first part of this project, the axolotl skin was completely decellularized to remove any potential antigens, specifically the major histocompatibility complex on the surface of the cells that may cause an immune reaction. Clearly, the results indicated that the Decellularized axolotl skin ECM of axolotls is well tolerated by mice, as no rejection occurred. The axolotl group that received the decellularized Axolotl Skin ECM demonstrated high reepithelialization, cellular density, collagen content (in a porous pattern similar to what is seen in intact skin), vascularization (angiogenesis) compared to Perioderm and control groups. Even the presence of hair follicles, which was not present in Perioderm and control groups, were observed in the axolotl group. Contrary to Perioderm and control groups, the new collagen formed under Decellularized Axolotl Skin ECM in the axolotl group seem to be in present at higher levels and be more porous or organized like that of intact tissue. In addition, it also looks as if there is a greater number of cells in the axolotl group. As compared with the Perioderm and control groups, wound sites with decellularized Axolotl Skin ECM showed the greatest amount of wound tissue formation. The basic hypothesis seems to be correct in that an ECM from a strong regenerator improves wound healing in a non-regenerating model. If future studies confirm our results this could represent a breakthrough in the development of biomaterials capable of stimulating regeneration in normally non-regenerating animals.

BIBLIOGRAPHY

1. Lazarus GS, Cooper DM, Knighton DR, Margolis DJ, Percoraro RE, Rodeheaver G, et al. Definitions and guidelines for assessment of wounds and evaluation of healing. Wound repair and regeneration. 1994;2(3):165-70.
2. Sorg H, Tilkorn DJ, Hager S, Hauser J, Mirastschijski U. Skin wound healing: an update on the current knowledge and concepts. European Surgical Research. 2017;58(1-2):81-94.
3. Yousef H, Alhajj M, Sharma S. Anatomy, skin (integument), epidermis. 2017.
4. Donati G, Watt FM. Stem cell heterogeneity and plasticity in epithelia. Cell stem cell. 2015;16(5):465-76.
5. Montagna W. The structure and function of skin: Elsevier; 2012.
6. Uitto J, Mauviel A, McGrath J. The dermal-epidermal basement membrane zone in cutaneous wound healing. The molecular and cellular biology of wound repair: Springer; 1988. p. 513-60.
7. Kolarsick PA, Kolarsick MA, Goodwin C. Anatomy and physiology of the skin. Journal of the Dermatology Nurses' Association. 2011;3(4):203-13.
8. Elder DE. Lever's histopathology of the skin: Lippincott Williams & Wilkins; 2014.
9. Rieger S, Zhao H, Martin P, Abe K, Lisse TS. The role of nuclear hormone receptors in cutaneous wound repair. Cell biochemistry and function. 2015;33(1):1-13.
10. Stadelmann WK, Digenis AG, Tobin GR. Physiology and healing dynamics of chronic cutaneous wounds. The American Journal of Surgery. 1998;176(2):26S-38S.
11. Wallace HA, Basehore BM, Zito PM. Wound healing phases. 2017.
12. Singer AJ, Clark RA. Cutaneous wound healing. New England journal of medicine. 1999;341(10):738-46.
13. Martin P. Wound healing--aiming for perfect skin regeneration. Science. 1997;276(5309):75-81.
14. Rasche H. Haemostasis and thrombosis: an overview. European Heart Journal Supplements. 2001;3(suppl_Q):Q3-Q7.
15. Versteeg HH, Heemskerk JW, Levi M, Reitsma PH. New fundamentals in hemostasis. Physiological reviews. 2013;93(1):327-58.
16. George Broughton I, Janis JE, Attinger CE. The basic science of wound healing. Plastic and reconstructive surgery. 2006;117(7S):12S-34S.
17. Cha J, Falanga V. Stem cells in cutaneous wound healing. Clinics in dermatology. 2007;25(1):73-8.
18. Gosain A, DiPietro LA. Aging and wound healing. World journal of surgery. 2004;28(3):321-6.
19. Profyris C, Tziotzios C, Do Vale I. Cutaneous scarring: Pathophysiology, molecular mechanisms, and scar reduction therapeutics: Part I. The molecular basis of scar formation. Journal of the American Academy of Dermatology. 2012;66(1):1-10.
20. Werner S, Grose R. Regulation of wound healing by growth factors and cytokines. Physiological reviews. 2003;83(3):835-70.
21. Midwood KS, Williams LV, Schwarzbauer JE. Tissue repair and the dynamics of the extracellular matrix. The international journal of biochemistry & cell biology. 2004;36(6):1031-7.

22. Madden JW, Peacock Jr EE. Studies on the biology of collagen during wound healing. 3. Dynamic metabolism of scar collagen and remodeling of dermal wounds. Annals of surgery. 1971;174(3):511.
23. Lau K, Paus R, Tiede S, Day P, Bayat A. Exploring the role of stem cells in cutaneous wound healing. Experimental dermatology. 2009;18(11):921-33.
24. Roh C, Lyle S. Cutaneous stem cells and wound healing. Pediatric research. 2006;59(4):100-3.
25. Eckes B, Nischt R, Krieg T. Cell-matrix interactions in dermal repair and scarring. Fibrogenesis & tissue repair. 2010;3(1):1-11.
26. Barker TH. The role of ECM proteins and protein fragments in guiding cell behavior in regenerative medicine. Biomaterials. 2011;32(18):4211-4.
27. Tziotzios C, Profyris C, Sterling J. Cutaneous scarring: Pathophysiology, molecular mechanisms, and scar reduction therapeutics: Part II. Strategies to reduce scar formation after dermatologic procedures. Journal of the American Academy of Dermatology. 2012;66(1):13-24.
28. Gurtner GC, Evans GR. Advances in head and neck reconstruction. Plastic and reconstructive surgery. 2000;106(3):672-82.
29. Enoch S, Price P. Cellular, molecular and biochemical differences in the pathophysiology of healing between acute wounds, chronic wounds and wounds in the aged. World Wide Wounds. 2004;13:1-17.
30. Asuku ME, Ibrahim A, Ijekeye FO. Post-burn axillary contractures in pediatric patients: a retrospective survey of management and outcome. Burns. 2008;34(8):1190-5.
31. Egeland B, More S, Buchman SR, Cederna PS. Management of difficult pediatric facial burns: reconstruction of burn-related lower eyelid ectropion and perioral contractures. Journal of craniofacial surgery. 2008;19(4):960-9.
32. Hunt O, Burden D, Hepper P, Stevenson M, Johnston C. Self-reports of psychosocial functioning among children and young adults with cleft lip and palate. The Cleft Palate-Craniofacial Journal. 2006;43(5):598-605.
33. Monaco JL, Lawrence WT. Acute wound healing: an overview. Clinics in plastic surgery. 2003;30(1):1-12.
34. Yokoyama H, Kudo N, Todate M, Shimada Y, Suzuki M, Tamura K. Skin regeneration of amphibians: A novel model for skin regeneration as adults. Development, growth & differentiation. 2018;60(6):316-25.
35. Baum CL, Arpey CJ. Normal cutaneous wound healing: clinical correlation with cellular and molecular events. Dermatologic surgery. 2005;31(6):674-86.
36. Hu MS, Maan ZN, Wu J-C, Rennert RC, Hong WX, Lai TS, et al. Tissue engineering and regenerative repair in wound healing. Annals of biomedical engineering. 2014;42(7):1494-507.
37. Tam J, Wang Y, Vuong LN, Fisher JM, Farinelli WA, Anderson RR. Reconstitution of full-thickness skin by microcolumn grafting. Journal of tissue engineering and regenerative medicine. 2017;11(10):2796-805.
38. Robson MC, Steed DL, Franz MG. Wound healing: biologic features and approaches to maximize healing trajectories. Current problems in surgery. 2001;38(2):72-140.
39. Darby IA, Bisucci T, Pittet B, Garbin S, Gabbiani G, Desmoulière A. Skin flap-induced regression of granulation tissue correlates with reduced growth factor and increased metalloproteinase expression. The Journal of pathology. 2002;197(1):117-27.

40. Dabiri G, Tumbarello DA, Turner CE, Van De Water L. Hic-5 promotes the hypertrophic scar myofibroblast phenotype by regulating the TGF-β1 autocrine loop. Journal of Investigative Dermatology. 2008;128(10):2518-25.
41. Lorenz HP, Lin RY, Longaker MT, Whitby DJ, Adzick NS. The fetal fibroblast: the effector cell of scarless fetal skin repair. Plastic and reconstructive surgery. 1995;96(6):1251-9; discussion 60.
42. Lorenz HP, Whitby DJ, Longaker MT, Adzick NS. Fetal wound healing. The ontogeny of scar formation in the non-human primate. Annals of surgery. 1993;217(4):391.
43. Rendl M, Lewis L, Fuchs E. Molecular dissection of mesenchymal–epithelial interactions in the hair follicle. PLoS biology. 2005;3(11):e331.
44. Soo C, Hu F-Y, Zhang X, Wang Y, Beanes SR, Lorenz HP, et al. Differential expression of fibromodulin, a transforming growth factor-β modulator, in fetal skin development and scarless repair. The American journal of pathology. 2000;157(2):423-33.
45. Shizuru JA, Negrin RS, Weissman IL. Hematopoietic stem and progenitor cells: clinical and preclinical regeneration of the hematolymphoid system. Annu Rev Med. 2005;56:509-38.
46. Ziegels J. The melanocytes of the Axolotl. Their modifications during skin regeneration. Archives de biologie. 1971;82(3):407-28.
47. Hui FW, Smith AA. Degeneration of Leydig cells in the skin of the salamander treated with cholinolytic drugs or surgical denervation. Experimental neurology. 1976;53(3):610-9.
48. Wallace H. Vertebrate limb regeneration: Wiley New York; 1981.
49. Roy S, Gatien S. Regeneration in axolotls: a model to aim for! Experimental gerontology. 2008;43(11):968-73.
50. Sen CK. Human wounds and its burden: an updated compendium of estimates. Mary Ann Liebert, Inc., publishers 140 Huguenot Street, 3rd Floor New …; 2019.
51. Järbrink K, Ni G, Sönnergren H, Schmidtchen A, Pang C, Bajpai R, et al. The humanistic and economic burden of chronic wounds: a protocol for a systematic review. Systematic reviews. 2017;6(1):1-7.
52. Bayat A, McGrouther D, Ferguson M. Skin scarring. Bmj. 2003;326(7380):88-92.
53. Brown B, McKenna S, Siddhi K, McGrouther D, Bayat A. The hidden cost of skin scars: quality of life after skin scarring. Journal of Plastic, Reconstructive & Aesthetic Surgery. 2008;61(9):1049-58.
54. Al-Waiz MM, Al-Sharqi AI. Medium-depth chemical peels in the treatment of acne scars in dark-skinned individuals. Dermatologic surgery. 2002;28(5):383-7.
55. Goodman GJ, Van Den Broek A. The modified tower vertical filler technique for the treatment of post-acne scarring. Australasian Journal of Dermatology. 2016;57(1):19-23.
56. Bouzari N, Davis SC, Nouri K. Laser treatment of keloids and hypertrophic scars. International journal of dermatology. 2007;46(1):80-8.
57. Klumpar DI, Murray JC, Anscher M. Keloids treated with excision followed by radiation therapy. Journal of the American Academy of Dermatology. 1994;31(2):225-31.
58. Mustoe TA, Cooter RD, Gold MH, Hobbs F, Ramelet A-A, Shakespeare PG, et al. International clinical recommendations on scar management. Plastic and reconstructive surgery. 2002;110(2):560-71.
59. Shah M, Foreman DM, Ferguson MW. Control of scarring in adult wounds by neutralising antibody to transforming growth factor β. The Lancet. 1992;339(8787):213-4.

60. Occleston NL, Laverty HG, O'Kane S, Ferguson MW. Prevention and reduction of scarring in the skin by transforming growth factor beta 3 (TGFβ3): from laboratory discovery to clinical pharmaceutical. Journal of Biomaterials Science, Polymer Edition. 2008;19(8):1047-63.
61. Mac Neil S. What role does the extracellular matrix serve in skin grafting and wound healing? Burns. 1994;20:S67-S70.
62. Hynes RO. Integrins: versatility, modulation, and signaling in cell adhesion. Cell. 1992;69(1):11-25.
63. Raghow R. The role of extracellular matrix in postinflammatory wound healing and fibrosis. The FASEB journal. 1994;8(11):823-31.
64. Diegelmann RF, Evans MC. Wound healing: an overview of acute, fibrotic and delayed healing. Front biosci. 2004;9(1):283-9.
65. Zielins ER, Atashroo DA, Maan ZN, Duscher D, Walmsley GG, Hu M, et al. Wound healing: an update. Regenerative medicine. 2014;9(6):817-30.
66. Wainwright D. Use of an acellular allograft dermal matrix (AlloDerm) in the management of full-thickness burns. Burns. 1995;21(4):243-8.
67. Tenenhaus M, Rennekampff H-O. Current concepts in tissue engineering: skin and wound. Plastic and reconstructive surgery. 2016;138(3S):42S-50S.
68. Daar DA, Gandy JR, Clark EG, Mowlds DS, Paydar KZ, Wirth GA. Plastic surgery and acellular dermal matrix: highlighting trends from 1999 to 2013. World journal of plastic surgery. 2016;5(2):97.
69. Walters J, Cazzell S, Pham H, Vayser D, Reyzelman A. Healing rates in a multicenter assessment of a sterile, room temperature, acellular dermal matrix versus conventional care wound management and an active comparator in the treatment of full-thickness diabetic foot ulcers. Eplasty. 2016;16.
70. Brockes JP. Amphibian limb regeneration: rebuilding a complex structure. Science. 1997;276(5309):81-7.
71. Brockes JP, Kumar A. Comparative aspects of animal regeneration. Annual review of cell and developmental biology. 2008;24:525-49.
72. Nacu E, Tanaka EM. Limb regeneration: a new development? Annual review of cell and developmental biology. 2011;27:409-40.
73. Lévesque M, Villiard É, Roy S. Skin wound healing in axolotls: a scarless process. Journal of Experimental Zoology Part B: Molecular and Developmental Evolution. 2010;314(8):684-97.
74. McCusker C, Bryant SV, Gardiner DM. The axolotl limb blastema: cellular and molecular mechanisms driving blastema formation and limb regeneration in tetrapods. Regeneration. 2015;2(2):54-71.
75. Seifert AW, Monaghan JR, Voss SR, Maden M. Skin regeneration in adult axolotls: a blueprint for scar-free healing in vertebrates. PloS one. 2012;7(4):e32875.
76. Denis J-F, Lévesque M, Tran SD, Camarda A-J, Roy S. Axolotl as a model to study scarless wound healing in vertebrates: role of the transforming growth factor beta signaling pathway. Advances in wound care. 2013;2(5):250-60.
77. Yokoyama H, Maruoka T, Aruga A, Amano T, Ohgo S, Shiroishi T, et al. Prx-1 expression in Xenopus laevis scarless skin-wound healing and its resemblance to epimorphic regeneration. Journal of Investigative Dermatology. 2011;131(12):2477-85.
78. Mu L, Tang J, Liu H, Shen C, Rong M, Zhang Z, et al. A potential wound-healing-promoting peptide from salamander skin. The FASEB Journal. 2014;28(9):3919-29.

79. Liu H, Mu L, Tang J, Shen C, Gao C, Rong M, et al. A potential wound healing-promoting peptide from frog skin. The international journal of biochemistry & cell biology. 2014;49:32-41.
80. Piccolo NS, Piccolo MS, Piccolo MS. The use of frogskin as a biological dressing for temporary cover of burn wounds. Innovations in plastic and aesthetic surgery: Springer; 2008. p. 129-37.
81. Longaker MT, Adzick NS. The biology of fetal wound healing: a review. Plastic and reconstructive surgery. 1991;87(4):788-98.
82. Longaker MT, Chiu ES, Adzick NS, Stern M, Harrison MR, Stern R. Studies in fetal wound healing. V. A prolonged presence of hyaluronic acid characterizes fetal wound fluid. Annals of surgery. 1991;213(4):292.
83. Seifert AW, Kiama SG, Seifert MG, Goheen JR, Palmer TM, Maden M. Skin shedding and tissue regeneration in African spiny mice (Acomys). Nature. 2012;489(7417):561-5.
84. Bruck SD. Biomaterials in medical devices. ASAIO Journal. 1972;18(1):1-8.
85. Badylak SF. Regenerative medicine and developmental biology: the role of the extracellular matrix. The Anatomical Record Part B: The New Anatomist: An Official Publication of the American Association of Anatomists. 2005;287(1):36-41.
86. Badylak SF, Freytes DO, Gilbert TW. Extracellular matrix as a biological scaffold material: structure and function. Acta biomaterialia. 2009;5(1):1-13.
87. Renth AN, Detamore MS. Leveraging “raw materials” as building blocks and bioactive signals in regenerative medicine. Tissue Engineering Part B: Reviews. 2012;18(5):341-62.
88. Vorotnikova E, McIntosh D, Dewilde A, Zhang J, Reing JE, Zhang L, et al. Extracellular matrix-derived products modulate endothelial and progenitor cell migration and proliferation in vitro and stimulate regenerative healing in vivo. Matrix Biology. 2010;29(8):690-700.
89. Zaman MH, Matsudaira P, Lauffenburger DA. Understanding effects of matrix protease and matrix organization on directional persistence and translational speed in three-dimensional cell migration. Annals of biomedical engineering. 2007;35(1):91-100.
90. Eweida A, Marei M. Naturally occurring extracellular matrix scaffolds for dermal regeneration: do they really need cells? BioMed research international. 2015;2015.
91. Kissane NA, Itani KM. A decade of ventral incisional hernia repairs with biologic acellular dermal matrix: what have we learned? Plastic and reconstructive surgery. 2012;130(5S-2):194S-202S.
92. Diegelmann RF, Dunn JD, Lindblad WJ, Cohen IK. Analysis of the effects of chitosan on inflammation, angiogenesis, fibroplasia, and collagen deposition in polyvinyl alcohol sponge implants in rat wounds. Wound Repair and Regeneration. 1996;4(1):48-52.
93. Lévesque M, Gatien S, Finnson K, Desmeules S, Villiard E, Pilote M, et al. Transforming growth factor: β signaling is essential for limb regeneration in axolotls. PloS one. 2007;2(11):e1227.
94. Christensen RN, Tassava RA. Apical epithelial cap morphology and fibronectin gene expression in regenerating axolotl limbs. Developmental dynamics: an official publication of the American Association of Anatomists. 2000;217(2):216-24.
95. Levin BP, Chu SJ. Changes in periimplant soft tissue thickness with bone grafting and dermis allograft: A case series of 15 consecutive patients. Int J Periodontics Restorative Dent. 2018;38(5):719-27.
96. Rubinstein S, Levin BP, Fulreader A, Barack D, Fujiki T. Prosthetic and Surgical Management of Atypical Space When Teeth Are Missing. Compendium of continuing education in dentistry (Jamesburg, NJ: 1995). 2019;40(6):358-66.

97. Lévesque M, Guimond JC, Pilote M, Leclerc S, Moldovan F, Roy S. Expression of heat-shock protein 70 during limb development and regeneration in the axolotl. Developmental dynamics: an official publication of the American Association of Anatomists. 2005;233(4):1525-34.
98. Ren H, Shi X, Tao L, Xiao J, Han B, Zhang Y, et al. Evaluation of two decellularization methods in the development of a whole-organ decellularized rat liver scaffold. Liver International. 2013;33(3):448-58.
99. Murphy CM, O'Brien FJ. Understanding the effect of mean pore size on cell activity in collagen-glycosaminoglycan scaffolds. Cell adhesion & migration. 2010;4(3):377-81.
100. Murphy CM, Haugh MG, O'brien FJ. The effect of mean pore size on cell attachment, proliferation and migration in collagen–glycosaminoglycan scaffolds for bone tissue engineering. Biomaterials. 2010;31(3):461-6.
101. Harley BA, Kim H-D, Zaman MH, Yannas IV, Lauffenburger DA, Gibson LJ. Microarchitecture of three-dimensional scaffolds influences cell migration behavior via junction interactions. Biophysical journal. 2008;95(8):4013-24.
102. Crapo PM, Gilbert TW, Badylak SF. An overview of tissue and whole organ decellularization processes. Biomaterials. 2011;32(12):3233-43.
103. Keane TJ, Londono R, Turner NJ, Badylak SF. Consequences of ineffective decellularization of biologic scaffolds on the host response. Biomaterials. 2012;33(6):1771-81.
104. Fadini GP, Spinetti G, Santopaolo M, Madeddu P. Impaired regeneration contributes to poor outcomes in diabetic peripheral artery disease. Arteriosclerosis, thrombosis, and vascular biology. 2020;40(1):34-44.
105. Koch S, Claesson-Welsh L. Signal transduction by vascular endothelial growth factor receptors. Cold Spring Harbor perspectives in medicine. 2012;2(7):a006502.
106. Marcelo KL, Goldie LC, Hirschi KK. Regulation of endothelial cell differentiation and specification. Circulation research. 2013;112(9):1272-87.
107. Wang Y, Armato U, Wu J. Targeting tunable physical properties of materials for chronic wound care. Frontiers in Bioengineering and Biotechnology. 2020;8:584.
108. Yang S, Leong K-F, Du Z, Chua C-K. The design of scaffolds for use in tissue engineering. Part I. Traditional factors. Tissue engineering. 2001;7(6):679-89.
109. Zeltinger J, Sherwood JK, Graham DA, Müeller R, Griffith LG. Effect of pore size and void fraction on cellular adhesion, proliferation, and matrix deposition. Tissue engineering. 2001;7(5):557-72.
110. Van Tienen TG, Heijkants RG, Buma P, de Groot JH, Pennings AJ, Veth RP. Tissue ingrowth and degradation of two biodegradable porous polymers with different porosities and pore sizes. Biomaterials. 2002;23(8):1731-8.
111. Wang W, Zhou G, Hu MC-T, Yao Z, Tan T-H. Activation of the hematopoietic progenitor kinase-1 (HPK1)-dependent, stress-activated c-Jun N-terminal kinase (JNK) pathway by transforming growth factor β (TGF-β)-activated kinase (TAK1), a kinase mediator of TGF β signal transduction. Journal of Biological Chemistry. 1997;272(36):22771-5.
112. Zhang YE. Non-Smad signaling pathways of the TGF-β family. Cold Spring Harbor perspectives in biology. 2017;9(2):a022129.
113. Sader F, Denis J-F, Laref H, Roy S. Epithelial to mesenchymal transition is mediated by both TGF-β canonical and non-canonical signaling during axolotl limb regeneration. Scientific Reports. 2019;9(1):1144.

APENDICES

The general protein analysis

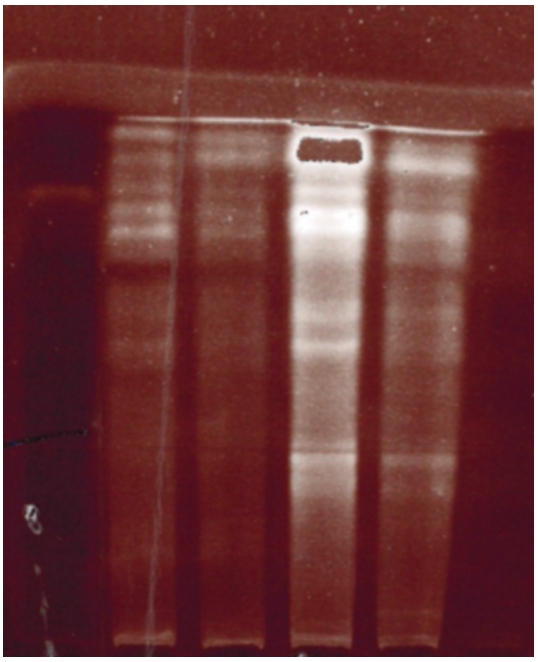

Figure 30 The general protein analysis was performed to determine and quantify the complete complement of proteins (the proteome) in both decellularized axolotl skin ECM and intact axolotl skin. It has been concluded that the general protein analysis revealed proteins that were readily visible in the decellularized axolotl skin ECM, indicating the decellularized axolotl skin ECM has been maintained after decellularization.